Heterogeneous & Homogeneous & Bio- & Nano-

CHEMCATCHEM

CATALYSIS

Accepted Article

Title: Elaborate Tuning in Ligand Makes Big Differences in Catalytic Performance: Bulky Nickel Catalysts for (Co)polymerization of Ethylene with Promising Vinyl Polar Monomers

Authors: Yanping Zhang, Hongliang Mu, Xuling Wang, Li Pan, and Yuesheng Li

To be cited as: *ChemCatChem* 10.1002/cctc.201900265

Link to VoR: http://dx.doi.org/10.1002/cctc.201900265

A Journal of

ChemPubSoc Europe

WILEY-VCH

www.chemcatchem.org

10.1002/cctc.201900265

WILEY-VCH

FULL PAPER

Elaborate Tuning in Ligand Makes Big Differences in Catalytic Performance: Bulky Nickel Catalysts for (Co)polymerization of Ethylene with Promising Vinyl Polar Monomers

Yanping Zhang,[a] Hongliang Mu,[b] Xuling Wang,[a] Li Pan,*[a] Yuesheng Li*[a]

Abstract: To reveal effect of electronic or steric modification of phosphino-phenolate nickel complex for preparing optimized catalysts, we take elaborated studies on structure-performance relationship by finely modifying substituents on *ortho*-phenoxy position or phosphorus moiety of this catalyst. It reveals that these newly synthesized complexes are thermally robust, and exhibits very high activity (up to 10^7 g·mol$_{Ni}^{-1}$·h^{-1}) in ethylene polymerization even at 120 °C. Associated with stoichiometric experiments, experimental results prove that nickel complexes bearing electron-withdrawing substituents on *ortho*-phenoxy position or electron-donating substituents on phosphorus atom show higher activity than contrastive catalysts toward ethylene polymerization and ethylene–methyl acrylate (MA) copolymerization. Among these catalysts, **3g** bearing a strong electron-withdrawing substituent on *ortho*-phenoxy position exhibits the highest activity, and produces copolymers with the highest molecular weight and analogous MA incorporation. Various challenging polar vinyl monomers, like polyethylene glycol monomethyl ether acrylate, can be efficiently copolymerized with ethylene.

Introduction

Late transition metal catalysts, bearing a low oxophilic metal center, play a vital role in coordination-insertion copolymerization of olefin and polar monomers which could produce high-valued polyolefin with improved surface properties.[1] In past decades, significant progresses have been achieved with the most representative palladium catalysts,[2] and various polar vinyl monomers have been effectively incorporated into polyethylene main chain.[3] However, molecular weight of such copolymers usually was severely suppressed to only several thousand by the polar group, made it far from application as a useful polymer material. Besides, cost of the palladium complex is still beyond industrial expectation.[2h] As a competitive candidate, low-cost nickel catalyst thus attracted increasing attention in both industry and academia.

Recently, nickel catalysts with various ligands, such as α-diimine nickel cationic catalyst,[4] phosphine-sulfonate neutral nickel catalyst,[5] salicylaldimine neutral nickel catalyst,[6] shell higher olefin process (SHOP) catalyst,[7] have contributed a lot to copolymerization of ethylene and various polar comonomer, respectively. However, only those comonomers bearing a spacer between C=C bond and polar group could be effectively incorporated. The commercially available polar comonomer, such as methyl acrylate (MA), with a polar group directly connected with the C=C bond usually leads to severe catalyst poisoning reaction.[8] To overcome this poisoning process, Chen group[8a] and Shimizu group[8c] designed nickel catalysts (**A** and **B** in Chart 1) that could copolymerize ethylene with MA by using transient interaction between metal center with other heteroatom, respectively. Chen *et al.* also designed several nickel catalysts based on rigid diphosphazane monoxide ligands of **C** (Chart 1), and those could copolymerize ethylene with MA.[8b] Catalysts **A** and **C** exhibited relative low catalytic activity (< 9.2 × 10^3 g mol$_{Ni}^{-1}$ h^{-1}) and produced copolymer with molecular weight lower than 20.7 × 10^3, MA incorporation of about 6.5 mol%. While catalyst **B** could only achieve ethylene–MA copolymerization under higher ethylene pressure (30 atm) and a large dosage of catalysts (80 μmol). By introducing an axial bulky group of neutral catalyst **D**, *β*-H elimination and biomolecular deactivation could be effectively suppressed. This neutral catalyst exhibited high catalytic activity (up to 10^5 g mol$_{Ni}^{-1}$ h^{-1}) toward ethylene–MA copolymerization and produced high-molecular-weight (M_w up to 108 × 10^3) copolymer with high MA incorporation (7.4 mol%).[9] However, it is very difficult for all ~~the~~ previously reported Ni catalysts to simultaneously achieve high catalytic activity and produce high-molecular-weight copolymer with good incorporation of polar unit.

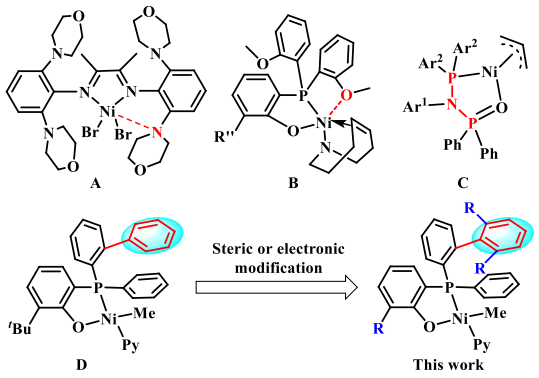

Chart 1. Representative nickel catalysts for ethylene and polar monomer copolymerization.

[a] Y. zhang, X. Wang, Prof. Dr. L. Pan and Prof. Dr. Y. Li
School of Material Science and Engineering and Collaborative Innovation Center of Chemical Science and Engineering (Tianjin)
Tianjin University
Tianjin 300072, China
E-mail: lilypan@tju.edu.cn; ysli@tju.edu.cn
[b] Dr. H.Mu
Polymer Composites Engineering Laboratory
Changchun Institute of Applied Chemistry, Chinese Academy of Sciences
Changchun 130022, China

Supporting information for this article is given via a link at the end of the document.

Generally, catalytic properties are sensitive to electronic or steric modification on its ligand.[6,7d-e,10-12] For example, Claverie[12] and Klabunde[7d,7e] proved that an electron-withdrawing substituent on the $C_{\alpha\text{-}P}$ or $C_{\beta\text{-}P}$ position of phosphors in SHOP-type catalyst was contributed to improving catalytic activity by two-orders-of-magnitude. In some cases, higher molecular-weight polyethylenes were obtained by introducing electron-withdrawing substituents.[11b,13] For example, fluorine atom as an electron-withdrawing substituent made a big difference on the high molecular weight becuase of C−H···F−C interaction.[13a-c] However, there was no clear trend between catalytic properties and catalyst structures by tuning the electronic effect in some reports.[14a-c] Chen[14d] also observed that different position of the substituents also played an important role. Grubbs[6] and Li[10a] *et al.* reported that neutral salicylaldiminato nickel catalyst bearing a bulky substituent on *ortho*-phenoxy position displayed high catalytic activity toward ethylene polymerization, and also produced high-molecular-weight polymers. Mecking and his coworkers also demonstrated that introducing an electron-withdrawing remote substituent on N-aryl moiety substantially enhanced the molecular weight and crystallinity of obtained polyethylene.[11] Additionally, Heinicke *et al.* showed that substituents on phosphorus atom played a key role on the catalytic properties of SOHP-type catalyst, especially molecular weight of polymer.[15] In a word, it is noteworthy that electronic or steric effect always plays different roles in different catalyst systems, and the influence of electronic or steric modification is always intricate because of diverse structural coordination environments. In addition, neutral nickel catalysts as single-component catalysts are of great academic and industrial interest benefiting from their labile ligands, such as pyridine, triphenylphosphine, and dimethylsulfoxide, becuause they can initiate polymerization reaction without expensive borates or MAO as a cocatalyst.[6a,10a] Therefore, aiming to prepare optimized netural catalysts with high thermostability, catalytic activity, copolymerization capability and good tolerance toward polar group, we carried out in depth exploration on effect of electronic or steric modification at different position of the frame of the promising catalyst **D**.

Results and Discussion

Ligands and Complexes Syntheses. Phosphino-phenolate ([P,O]) ligands with different electronic and steric substituents at *ortho*-position of the *oxygen* donor were synthesized as presented in Scheme 1. Tetrahydropyranyl (THP) ether compounds **a**–**g** were lithiated by *n*-BuLi, and then reacted with PAr_1PhCl (Ar_1 = 2-(2',6'-$(MeO)_2$-C_6H_3)-C_6H_4), thus obtaining compounds **1a**–**g**, respectively. Protective group (THP) of complexes **1a**–**g** could be easily removed to afford ligands **2a**–**g** by adding drops of hydrochloric acid. In the case of ligand **2g**, introduction of $–C_6F_5$ substituent was accomplished after introduction of –PArPh moiety by F-Li exchange reaction. Ligand **2h** was prepared via a procedure similar to **2a** using PAr_2PhCl instead of PAr_1PhCl. Complex PAr_1PhCl (Ar_1 = 2-(2',6'-$(MeO)_2$-C_6H_3)-C_6H_4) was synthesized according to literature,[9] while synthesis of PAr_2PhCl (Ar_2 = 2-(2',6'-F_2-C_6H_3)-C_6H_4) was described in Supporting Information.

As far as we know, electronic modification on *ortho*-phenoxy position makes a difference on the electric density of hydrogen atom in phenolic hydroxyl group. Presence of an electron-withdrawing group at *ortho*-position of phenolic hydroxyl group will decrease electric density of hydrogen atom, thus the resonance of –O*H* in ^{1}H NMR spectrum shifts to low field. As observed, chemical shifts of the hydroxyl proton from each ligand with different substituent at *ortho*-position of the phenyl are in following sequence: **2b** (9.65 ppm) > **2a** (9.46 ppm), **2d** (9.24 ppm) > **2c** (8.33 ppm), **2g** (8.98 ppm) > **2f** (8.28 ppm).

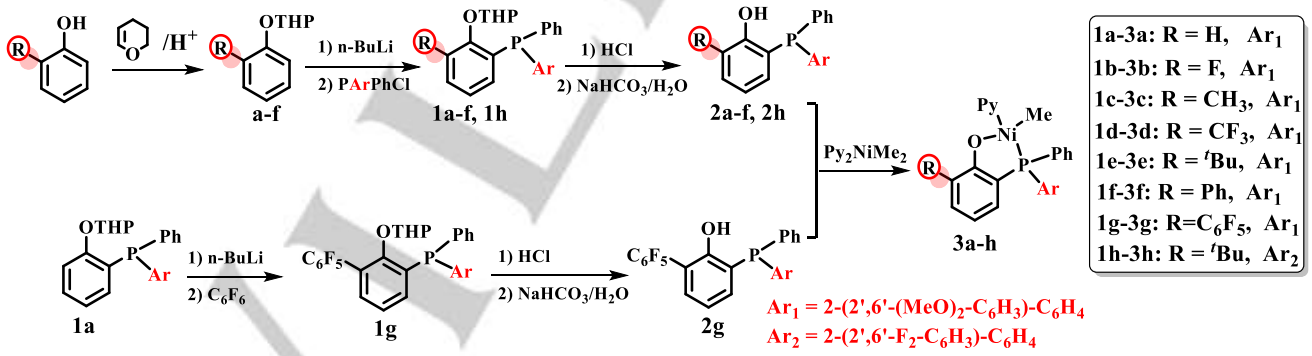

Scheme 1. Synthesis of ligands **2a**–**h** and corresponding nickel complexes **3a**–**h**.

Nickel complexes **3a**–**h** were synthesized by a facile one-step reaction of corresponding phosphino-phenolate ligand **2a**–**h** with Py_2NiMe_2 in good yields (> 80%) as depicted in Scheme 1. All nickel complexes were characterized by elemental analysis and NMR spectroscopy. Presence of doublet peaks at negative field in ^{1}H NMR spectra, which is originated from spin-spin coupling between the protons of Ni–C*H*$_3$ and phosphorus atom, proves that the phosphorus atom is coordinated to the Ni center. One doublet peak can be observed in ^{31}P NMR spectrum for complex **3b** because of the long-range spin-spin coupling between

phosphorus and fluorine atom, while one singlet is deteceted for all other complexes. It is also observed that resonances for complexes with electron-withdrawing substituents on *ortho*-phenoxy position (**3b**: 20.80, **3d**: 19.92, **3g**: 20.39 ppm, Figure 1) slightly shift to higher field compared to the corresponding electron-donating complex (**3a**: 21.09, **3c**: 21.27, **3f**: 21.28 ppm) in ^{31}P NMR spectra. This observation may be explained by that introducing an electron-withdrawing substituent on *ortho*-phenoxy position makes the metal center more electron-deficient, both σ-donating of phosphine ligand and back donating bonding between p_z orbital of nickel center and empty d_π orbital of phosphorus atom are therefore slightly weaken. Electronic density of phosphorus atom is decreased by introducing an electron-withdrawing substituent, as observed, corresponding resonance for electron-poor complex **3h** (24.68 ppm) in ^{31}P NMR spectrum evidently shifts to lower field compared to electron-efficient **3e** (21.47 ppm).

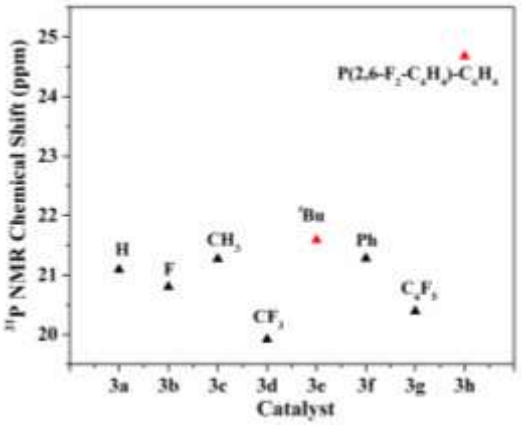

Figure 1. Chemical shifts of phosphorus atom for nickel complexes **3a**–**h** in ^{31}P NMR spectra.

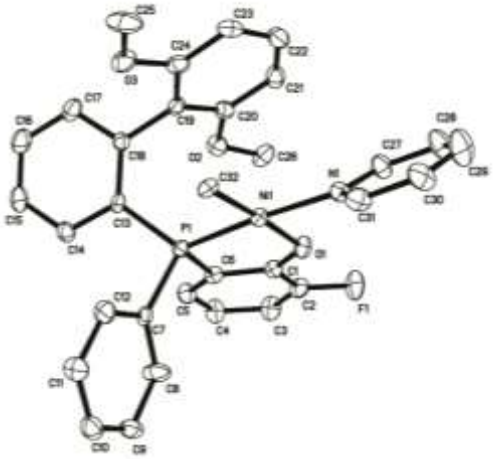

Figure 2. ORTEP plot of complex **3b**. Ellipsoids are shown with 30% probability. Hydrogen atoms are omitted for clarity. Selected bond lengths (Å) and angles (°): Ni(1)–O(1) 1.9314(16), Ni(1)–N(1) 1.9565(19), Ni(1)–P(1) 2.1206(6), Ni(1)–C(32) 1.967(2), Ni(1)–O(2) 3.817, Ni(1)–O(3) 4.436. O(1)–Ni(1)–N(1) 88.69(7), O(1)–Ni(1)–C(32) 177.57(8), N(1)–Ni(1)–C(32) 92.43(9), O(1)–Ni(1)–P(1) 87.56(5), N(1)–Ni(1)–P(1) 175.58(6), C(32)–Ni(1)–P(1) 91.23(7).

Nickel complexes **3b**, **3d** and **3h** were also exemplified by X-ray diffraction analyses (**3b** and **3h** is in Figure 2–3, respectively, **3d** is in Figure S87). Generally, nickel center adopts a distorted square-planner geometry, and labile ligand pyridine is located *trans* to the phosphorus atom because of 'trans effect'.[9] As described in Figure 2 and 3, either bulky 2-(2,6-$(OCH_3)_2C_6H_3)C_6H_4$– or 2-(2,6-F_2-$C_6H_3)C_6H_4$– group effectively shields the nickel center from axial position. Note that bond length of Ni(1)–O(2) and Ni(1)–O(3) in **3b** is 3.817 and 4.436 Å, respectively, either is longer than the sum of the van der Waals radii of nickel and oxygen (3.15 Å).[16] In addition, bond length of Ni(1)–F(1) and Ni(1)–F(2) in **3h** is 3.791 and 4.487 Å, respectively, while the sum of van der Waals radii between Ni and F atom is 3.31 Å.[17] This result reveals that the interaction between –F or –OMe group and the nickel center for both **3b** and **3h** is negligible.

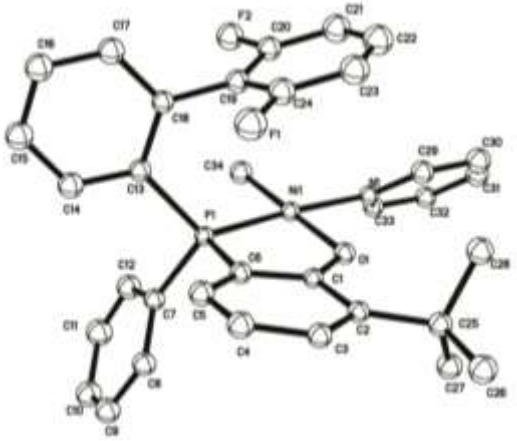

Figure 3. ORTEP plot of complex **3h**. Ellipsoids are shown with 30% probability. Hydrogen atoms are omitted for clarity. Selected bond lengths (Å) and angles (°): Ni(1)–O(1) 1.928(2), Ni(1)–N(1) 1.955(3), Ni(1)–P(1) 2.1080(11), Ni(1)–C(34) 1.944(4), Ni(1)–F(1) 3.791, Ni(1)–F(2) 4.487. O(1)–Ni(1)–C(34) 179.67(15), O(1)–Ni(1)–N(1) 88.75(11), C(34)–Ni(1)–N(1) 91.58(15), O(1)–Ni(1)–P(1) 86.68(8), C(34)–Ni(1)–P(1) 92.99(12), N(1)–Ni(1)–P(1) 175.18(10).

Ethylene polymerization studies. Because of the great academic and industrial interest, neutral [P,O] chelate cayalysts **3a**-**h** were applied as single-component catalysts to promote ethylene polymerization without any activator or scavenger at 10 bar of ethylene pressure under 80 °C. As shown in Table 1, catalytic activity is markedly increased (entry 1 *vs* 2, 3 *vs* 4, and 6 *vs* 7) by introducing an electron-withdrawing substituent (–F, $–CF_3$ or $–C_6F_5$) on *ortho*-phenoxy position. The most electron-deficient complex **3g** bearing a $–C_6F_5$ group exhibits the highest catalytic activity among complexes **3a**–**d**, **3f** and **3g**. Introduction of an electron-withdrawing group on *ortho*-phenoxy position makes the nickel center more electrophilic, and thus ethylene more easily coordinating to it. Additionally, a steric bulky group on *ortho*-phenoxy position also contributes to an increased catalytic activity. Comparing the polymerization results of complexes **3a**, **3c** and **3e** will give us more insight into the effect of steric bulk. Complex **3e** bearing the bulkiest substituent (6-^{t}Bu) exhibits the highest catalytic activity (up to 24.06×10^6 g_{PE} mol_{Ni}^{-1} h^{-1}, entry 5), while complex **3a** shows the lowest catalytic activity of 3.54×10^6 g_{PE}

mol_{Ni}^{-1} h^{-1}. In the case of complexes **3b**, **3d** and **3g**, the similar trend can be observed that complex **3g** bearing the bulkiest substituent (6-C_6F_5) exhibits the highest catalytic activity (up to 17.04 × 10^6 g_{PE} mol_{Ni}^{-1} h^{-1}, entry 7). It also indicates that a bulky group can help to enhance the steric hindrance around the active Ni site, thus the labile ligand pyridine (Py) readily dissociates from Ni center, and then ethylene can easily go close to the Ni center.

Besides catalytic activities, molecular weights of the obtained polymers can also be well controlled by tuning ligand structure of Ni complex. In comparison of complex **3a** with **3b**, molecular weight of resultant polymer decreases from 169.3 × 10^3 to 83.8 × 10^3 (entry 1 *vs* entry 2, Table 1). Similar observations can also be found in comparison between **3c** and **3d** (entry 3 *vs* 4, from 120.3 × 10^3 to 36.0 × 10^3) or **3f** and **3g** (entry 6 *vs* 7, from 74.8 × 10^3 to 53.7 × 10^3). All above comparisons reveal that molecular weight of the synthesized polyethylene is declined by introducing an electron-withdrawing substituent on *ortho*-phenoxy position, such as –F, $–CF_3$ or $–C_6F_5$ group, and this feature is in good accordance with some previous reports.[15, 18, 19] However, higher molecular weight polyethylene was obtained with an electron-withdrawing substituent in some other reports.[11b,13] We speculate the different influence trend originates from different ligand skeleton. Generally, molecular weight of the obtained polyethylene depends on the ratio of ethylene insertion rate relative to chain transfer rate and chain termination rate. We thus speculate that the decrease in molecular weight is originated from the facilitated reductive elimination (*β*-H elimination) rate relative to ethylene insertion rate by introducing an electron-withdrawing substituent.[20]

Table 1. Data of ethylene polymerization using neutral nickel catalysts **3a**–**h**.[a]

Entry	Cat.	Yield (g)	Act.[b] (10^3)	TOF[c] (10^3)	M_n[d] (10^3)	M_w [d] (10^3)	M_w/M_n [d]	T_m [e] (°C)
1	**3a (H)**	5.9	3540	126	74.4	169.3	2.3	134.4
2	**3b (F)**	17.3	10380	370	38.1	83.8	2.2	132.6
3	**3c (CH_3)**	12.9	7740	276	30.4	120.3	3.9	135.2
4	**3d (CF_3)**	24.1	14460	516	9.3	36.0	3.9	128.5
5	**3e (^{t}Bu)**	40.1	24060	859	18.1	43.6	2.4	130.0
6	**3f (Ph)**	23.5	14100	504	36.9	74.8	2.0	129.6
7	**3g (C_6F_5)**	28.4	17040	609	23.4	53.7	2.3	127.0
8	**3h (P-F)**	33.7	20220	722	13.2	29.2	2.2	131.1

[a] 100 mL of toluene, 5 μmol of catalyst, 20 min, 10 bar of ethylene, 80 °C. [b] In unit of g_{PE} mol_{Ni}^{-1} h^{-1}. [c] TOF, turnover frequency, in unit of 10^3 mol_{PE} mol_{Ni}^{-1} h^{-1}, E, ethylene. [d] Determined by GPC in 1,2,4-trichlorobenzene at 150 °C *vs* narrow polystyrene standard. [e] Determined by DSC, the second heating curve at the rate of 20 °C min^{-1}.

Influence of phosphine moiety electronic modification on catalytic performance is also explored. Both catalytic activity and molecular weight of polyethylene are decreased by introducing an electron-withdrawing substituent on phosphine moiety. Comparing the data of complex **3e** and **3h** in Table 1, catalytic activity is decreased from 24.06 × 10^6 to 20.22 × 10^6 g_{PE} mol_{Ni}^{-1} h^{-1}. The molecuar weight of polyethene produced by **3e** and **3f** is 43.6 × 10^3 and 29.2 × 10^3, respectively. This observation is reasonable because basicity of phosphine moiety is decreased by introducing an electron-withdrawing substituent, and '*trans* effects' become weaker, thus making the liable ligand pyridine binds more tightly to Ni center and decelerating the coordination-insertion process.

Most previously reported nickel catalysts tended to decompose beyond 60 °C,[21] while high reaction temperature (70–115 °C) was essential condition for industrial gas-phase olefin polymerizations.[22] To reveal the influences of reaction temperature on catalytic performances and evaluate the thermal stability of the representative catalyst, we conducted polymerization under different temperatures at 10 bar of ethylene using complex **3e** (Table 2). Surprisingly, **3e** is very active toward ethylene polymerization in a very wide temperature window. As the temperature elevated from 20 to 80 °C, the catalytic activity is dramatically enhanced from 2.88 × 10^6 to 24.06 × 10^6 g_{PE} mol_{Ni}^{-1} h^{-1} (entries 1–4). When reaction temperature further elevated from 80 to 140 °C, catalytic activity is decreased to 2.76 × 10^6 g_{PE} mol_{Ni}^{-1} h^{-1}, which is very similar to that of polymerization at 20 °C. It is notable that even at very high temperature of 120 °C, catalyst **3e** still displays extremely high catalytic activity (up to 13.1 × 10^6 g_{PE} mol_{Ni}^{-1} h^{-1}), and besides, yields polyethylene with relatively high molecular weight (17.4 × 10^3). To our best knowledge, this is the most thermally stable neutral nickel catalyst reported so far.[15, 19b, 21c, 22a, 22b] Molecular weight of resultant polyethylene is closely related to reaction temperature. As displayed in Table 2, polymerization can be initiated under 20 °C, and polyethylene with very high molecular weight of 632.4 × 10^3 can be obtained with narrow polydispersity index of 1.8. The highest molecular weight of 717.1 × 10^3 emerges at 40 °C, then it is slightly decreased with enhancement of reaction temperature till 60 °C. This catalyst simultaneously possesses high catalytic activity and produces high-molecular-weight polymer, and it is a very promising breakthrough compared to all previously reported examples.[21b, 21c, 22a] Further enhancement in reaction temperature from 60 to 140 °C accelerates the decrease in molecular weight, but the lowest ~~weight average~~ molecular weight is still relatively high (> 10 × 10^3). Decrease in molecular weight dominatingly results from the facilitated rates of chain transfer reaction at elevated temparatures.

In addition, We also carry out ethylene polymerization at 120 °C using catalyst **3d** bearing a strong electron-withdrawing substituent $–CF_3$ and the bulkeir catalyst **3g** bearing another strong electron-withdrawing substituent $–C_6F_5$. These two catalysts show very high catalytic activity, and the bulkeir **3g** shows higher catalytic activity than **3d** (Table 2, entry 8 vs 9). We aslo explore the thermal stability of these nickel catalysts at longer polymerization period under 120 °C. The selected catalyst **3e** shows increased catalytic activity and molecular weitht of polymer with prolonged reaction time at 30 °C (Table S2, entry S5-S8). Ethylene polymerization is also conducted with prolonged reaction time at 120 °C using lower catalyst concentration to avoid catalyst being enwrapped. As shown in the plots of TOF-time (Figure S86), the TOF remains very similar value (134 × 10^3**–**144 × 10^3). To further explore the thermostability of catalyst **3e**, we also first carried out ethylene polymerization at 120 °C for 10 min, then shutted off the ethylene gas for 20 or 40 min, respectively,

after that, charged the ethylene gas again to trigger the polymerization for another 10 min. To our delight, after this intermittent process, catalyst **3e** still exhibits comparable catalytic activity with the data of direct reaction for 20 min in Table 2, entry 6. All these data domenstrate that catalyst **3e** exhibits excellent thermal stability. All resultant polyethylene possesses highly linear structure or only very few methyl branches (4/1000C) produced at temperature over 120 °C as evidenced by ^{13}C NMR (Figure S62–63) and differential scanning calorimetry (DSC) analyses (T_m = 126.2–138.5 °C).

Table 2. Controlled ethylene polymerization by using catalyst **3e**.[a]

Entry	T (°C)	Yield (g)	Act.[b] (10^3)	TOF[c] (10^3)	M_n[d] (10^3)	M_w[d] (10^3)	M_w/M_n[d]	T_m[e] (°C)
1	20	4.8	2880	103	358.1	632.4	1.8	134.1
2	40	8.1	4860	173	552.8	717.1	1.3	138.5
3	60	20.1	12000	429	489.3	679.0	1.4	137.1
4	80	40.1	24060	859	18.1	43.6	2.4	130.0
5	100	22.0	13120	469	14.2	33.6	2.4	127.5
6[f]	120	21.6	12960	462	5.1	17.4	3.4	126.2
7[f]	140	4.6	2760	99	3.4	12.1	3.6	126.6
8[g]	120	16.6	9960	356	10.5	29.5	2.8	126.9
9[h]	120	18.9	11340	405	9.9	30.8	3.1	128.6

[a] 100 mL of toluene, 5 μmol of catalyst **3e**, 20 min, 10 bar of ethylene. [b] Unit of g_{PE} mol_{Ni}^{-1} h^{-1}. [c] TOF, turnover frequency, in unit of 10^3 mol_E mol_{Ni}^{-1} h^{-1}, E, ethylene. [d] Determined by GPC in 1,2,4-trichlorobenzene at 150 °C *vs* narrow polystyrene standard. [e] Determined by DSC, the second heating curve at the rate of 20 ˚C min^{-1}. [f] 100 mL of naphthane. [g] 100 mL of naphthane, 5 μmol of catalyst **3d**; [h] 100 mL of naphthane, 5 μmol of catalyst **3g**.

Reaction of nickel complex with methyl acrylate (MA). To understand the influence of steric or electronic modification on tolerance and reactivity of nickel complexes with polar monomer, reaction of different Ni complex (**3c–h**) with excess MA (60 equivalents of Ni) in the absence of ethylene were monitored by NMR technique at 25 °C, respectively. As revealed, MA inserts into Ni–CH_3 bond mainly *via* 2,1-fashion to form [P,O]Ni–$CH(CO_2CH_3)CH_2CH_3$ ([P,O]Ni–MA–CH_3) and the resonance intensity of Ni–CH_3 at negative field is accordlingly decreased.[9, 19a] The insertion product [P,O]Ni–MA–CH_3 can undergo *β*-H elimination to form free Ni–hydride and methyl crotonate. Accompanying bimolecular decomposition reaction simultaneously occurs via reaction of free Ni-hydride with [P,O]Ni–MA–CH_3. This decomposition reaction can be further evidenced by formation of methyl butyrate decomposition product. All ^1H NMR spectra of reaction of **3c–g** with MA after 2 h are presented in Figure 4. The residue resonances of Ni–CH_3 are still distinct even after 2 h, indicating that these nickel complexes exhibit excellent polar group tolerance. Besides, some new resonances present at 2.02, 1.51, and 0.76 ppm can be ascribed to the proton of –C$H_2$$CO_2$Me, –C$H_2$$CH_3$, and –C$H_3$, respectively. Characteristic resonances of [P,O]Ni–MA–CH_3 are not very prominent, and weak resonances at –0.29 and 0.36 ppm refer to Ni–$CH(CO_2CH_3)CH_2C$$H_3$ and Ni–$CH(CO_2CH_3)C$$H_2CH_3$ can be further affirmed by ^1H-^1H COSY (Supporting Information, Figure S51). These identifications suggest that above mentioned accompanying decomposition reaction occurred quickly, however these nickel complexes still display good tolerance to MA.

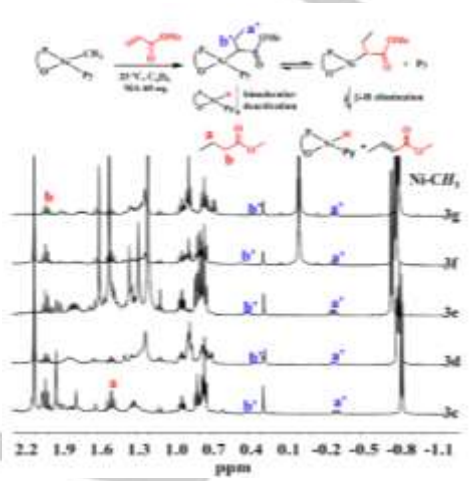

Figure 4. Selected ^1H NMR spectra (expanded 2.2 to -1.1 ppm) of reaction of nickel complexes **3c–g** with 60 equivalents of methyl acrylate after 2 h at 25 °C.

It is notable that apparent rate constant is the rate of equilibrium reaction as shown below [19a]:

$$[P,O]Ni(CH_3)(Py) + MA \rightleftarrows [P,O]Ni–MA–CH_3 + Py$$

Herein, the decay of Ni–CH_3 resonance is used to estimate the apparent rate constant of reaction between Ni complex and MA, and the decay rate of the Ni–CH_3 resonance is found to follow first-order kinetics at 25 °C (Figure 5). Note that electron-poor complex **3g** displays the lowest apparent rate constant (k_{app} = 3.94×10^{-5} s^{-1}), which is significantly lower than that of complex **3f**. Similarly, complex **3d** (k_{app} = 4.61×10^{-5} s^{-1}) bearing an electron-withdrawing –CF_3 group also displays a lower rate relative to **3c** (k_{app} = 13.17×10^{-5} s^{-1}). Evidently, electron-poor nickel complexes show a slower rate of MA insertion into Ni–CH_3 bond, in other words, the electron-poor nickel complexes show better tolerance in presence of excess MA. Additionally, complex **3e** bearing a bulkier group (6-*t*Bu) undergoes a slower reaction rate than complex **3c** (6-CH_3). The reactivity of nickel catalysts is decreased in sequence: **3g** > **3d** > **3f** > **3c**; **3e** > **3c**. Substituent on phosphorus atom also shows influence on reactivity in reaction of MA and Ni complex. For instance, Ni–CH_3 resonance of **3h** which is bearing 2',6'-F_2-substituted biphenyl group on P-aryl moiety nearly disappears after reaction for 13 h (Figure S85), while Ni–CH_3 resonance of **3e** which is bearing 2',6'-OMe_2-substituted biphenyl group on P-aryl moiety still exists after reaction for 38 h (Figure S82). It is evident that an electron-donating group on P-aryl moiety is helpful to enhance the catalyst tolerance toward polar MA. After reaction of nickel complex with MA for 30 h, the reaction mixture was also tried to initiate ethylene polymerization. Surprisingly, **3d** and **3g** bearing an electron-withdrawing substituent on *ortho*-phenoxy position still exhibits high catalytic activity (up to 1.56×10^6 g mol_{Ni}^{-1} h^{-1}, Table S1, entry S5) toward ethylene polymerization. This is a highly persuasive evidence to prove that introducing an electron-

withdrawing substituent on *ortho*-phenoxy position is an effective way to enhance tolerance of the Ni catalyst.

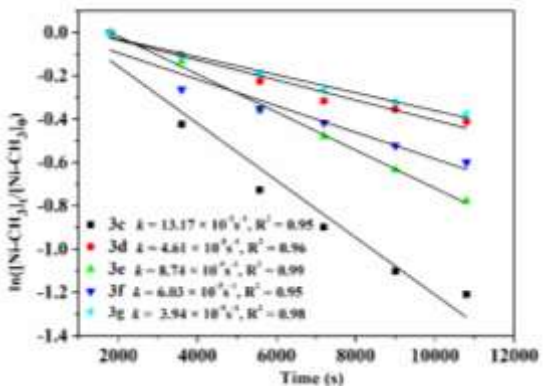

Figure 5. First order kinetic of the reaction of nickel complexes (**3c**–**g**) with 60 equivalents of methyl acrylate over 3 h: plots of decreasing intensity of resonance of Ni–C*H*$_3$ protons over time in ^{1}H NMR spectra.

Copolymerization of ethylene and methyl acrylate. Representative data of copolymerization of ethylene with methyl acrylate promoted by all nickel complexes are tabulated in Table 3. Both catalytic activity and molecular weight of the resultant copolymer are significantly increased by introducing an electron-withdrawing substituent (–F, –CF_3, or –C_6F_5) on *ortho*-phenoxy position. For example, catalytic activity of complex **3d** is much higher than that of **3c** (128 × 10^3 *vs* 37.2 × 10^3 g mol_{Ni}^{-1} h^{-1}, entry 4 *vs* 3), and molecular weight of copolymer yielded by complex **3d** is two times higher than that by complex **3c** (116.3 × 10^3 *vs* 43.3 × 10^3). Note that **3g** bearing an electron-withdrawing group –C_6F_5 shows the highest activity (up to 132 × 10^3 g mol_{Ni}^{-1} h^{-1}, entry 7) and produces highly linear copolymers with the highest molecular weight (M_w up to154 × 10^3, entry 7). In addition, the incorporation of MA is also affected by substituent type. The influence is not very obvious in the presence of low MA concentration. For instance, MA incorporation of copolymer by complex **3a** is 1.9 mol%, and this value is slightly higher than that by complex **3b** (1.6 mol%). Similar to this phenomena, complex **3d** (1.4 mol%) or **3g** (0.7 mol%) bearing a srtong electron-withdrawing substituent –CF_3 or –C_6F_5 on *ortho*-phenoxy position produces E-MA copolymer with lower MA incorporation than the corresponding complex **3c** (1.5 mol%) or **3f** (1.5 mol%). In the presence of high MA concentration, as can be observed (Table 3, 10 vs 11, 13 vs 14), the influnce of electronic effect was more obvious, and MA incorporation by a catalyst bearing an electron-withdrawing substituent on *ortho*-phenoxy position is also lower than that by contrastive catalysts. For example, MA incorporation of copolymer produced by electron-deficient complex **3d** and **3g** is 3.1 and 2.8 mol%, respectively, which is lower than that by complex **3c** (4.7 mol%, entry 10) and **3f** (3.6 mol%, entry 13). Ethylene is more nucleophilic to electron-deficient Ni center than electron-deficient olefin (MA), and a little smaller than MA, thus it is more easier for ethylene to insert into polymer chain during the coordination-insertion process.[2a, 3a, 23]

While introducing a bulky group on *ortho*-phenoxy position, both catalytic activity (3.9 × 10^3, 37.2 × 10^3, and 50.5 × 10^3 g mol_{Ni}^{-1} h^{-1} for **3a**, **3c** and **3e**, respectively) and molecular weight (10.6 × 10^3, 43.3 × 10^3 and 59.3 × 10^3 for **3a**, **3c** and **3e**, respectively) of the resultant copolymers are also enhanced.

Furthermore, electronic modification of phosphorus moiety also makes a dramatic effect on ethylene–MA copolymerization. It is revealed that electron-rich catalyst **3e** is more active than electron-poor catalyst **3h**, and **3e** also produces much higher molecular-weight copolymer (entry 5 *vs* 8, and 12 *vs* 15, respectively). For example, catalytic activity of ethylene/MA copolymerization by catalyst **3e** is up to 50.5 × 10^3 g mol_{Ni}^{-1} h^{-1} (entry 5), but catalytic activity by catalyst **3h** is only about 32.9 × 10^3 g mol_{Ni}^{-1} h^{-1} (entry 8). The molecular weight of obtained copolymers by catalysts **3e** and **3h** is 59.3 × 10^3 and 27.8 × 10^3, respectively. However, complex **3h** produces E-MA copolymer with higher MA incorporation than complex **3e** by 0.7 mol%.

Table 3. Copolymerization of ethylene and methyl acrylate (MA) by using catalysts **3a–h.**[a]

Entry	Cat.	[MA][b]	Yield (g)	Act.[c] (10^3)	Incorp.[d] (mol%)	M_w[e] (10^3)	PDI[e]	T_m[f] (°C)
1	**3a(H)**	0.1	0.039	3.9	1.9	10.6	1.8	125.2
2	**3b(F)**	0.1	0.075	7.5	1.6	21.5	1.8	126.6
3	**3c(CH_3)**	0.1	0.372	37.2	1.5	43.3	1.7	122.4
4	**3d(CF_3)**	0.1	1.280	128	1.4	116.3	2.2	121.6
5	**3e(^{t}Bu)**	0.1	0.505	50.5	2.0	59.3	2.0	123.3
6	**3f(Ph)**	0.1	0.400	40	1.5	56.9	1.8	121.3
7	**3g(C_6F_5)**	0.1	1.320	132	0.7	154.0	2.0	126.3
8	**3h(P-F)**	0.1	0.329	32.9	2.7	27.8	2.0	120.2
9	**3a(H)**	0.2	0.030	3.0	2.5	7.6	1.7	120.9
10	**3c(CH_3)**	0.2	0.179	17.9	4.7	14.4	1.8	113.6
11	**3d(CF_3)**	0.2	0.386	38.6	3.1	31.1	2.0	119.2
12[g]	**3e(^{t}Bu)**	0.2	0.263	26.3	2.2	22.6	2.0	117.0
13	**3f(Ph)**	0.2	0.140	14	3.6	26.0	2.1	113.7
14	**3g(C_6F_5)**	0.2	0.750	75.0	2.8	75.0	2.2	121.7
15	**3h(P-F)**	0.2	0.163	16.3	4.2	12.1	1.9	112.4
16[h]	**3f(Ph)**	0.2	0.052	5.2	6.1	8.9	1.7	106.2
17[h]	**3g(C_6F_5)**	0.2	0.210	210	3.9	18.0	2.0	114.3
18[i]	**3e(^{t}Bu)**	0.2	0.423	21.2	2.7	20.5	2.0	116.8

Polymerization conditions: [a] 50 mL of toluene, 10 μmol of catalyst, 60 min, 50 °C, 10 bar of ethylene. [b] units of mol L^{-1}. [c] In units of g mol_{Ni}^{-1} h^{-1}. [d] Determined by ^{1}H NMR spectroscopy at 120 °C. [e] PDI = M_w/M_n, determined by GPC in 1,2,4-trichlorobenzene at 150 °C *vs* narrow polystyrene standard. [f] Determined by DSC, the second heating curve at the rate of 20 °C min^{-1}. [g] Ref.[9]. [h] 5 bar. [i] Reaction for 120 min.

In a word, the catalytic activity and molecular weight of resultant copolymers increased in a sequence: **3g** > **3d** > **3f** > **3c** > **3b** > **3a**; **3e** > **3c** > **3a**; **3e** > **3h.** The enhanced catalytic activity and decreased insertion percentage of MA for catalysts bearing electronic-withdrawing substituents in the copolymerization of ethylene with MA could be also explained by a lower reaction rate of catalyst (Figure 6) with MA for electron-deficient catalyst. The sequence of catalytic activity is in good accordance with catalyst tolerance in the presence of excess MA. Furthermore, **3d** and **3g** bearing a strong electron-withdrawing substituent can simultaneously achieve high catalytic activity, and produce higher molecular weight copolymer with even higher MA incorporation than that of our previously reported **3e**, demonstrating that an excellent catalyst system for copolymerization of ethylene with

vinyl polar monomer can be achieved via elaborately tuning substituents on proper sites around Ni center.

As previously reported, MA incorporation could be enhanced with increasing MA feed concentration, while the molecular weight of copolymer was decreased, because *β*-H elimination was more facilitated after insertion an MA unit.[9, 19a] In the case of low MA concentrantion, for instence, catalyst **3g** bearing a strong electronic-withdrawing substituent $–C_6F_5$ on the *ortho*-phenoxy position displays very high catalytic activity (up to 132 × 10^3 g mol_{Ni}^{-1} h^{-1}, entry 7) and produces high molecular-weight copolymer (154.0 × 10^3), but MA incorporation in copolymer is only 0.7 mol%. Howerver, in the precense of higher MA concentration, MA incoropration in copolymer is increased from 0.7 to 2.8 mol%, while the catalytic activity significantly decreases to 75 × 10^3 g mol_{Ni}^{-1} h^{-1}, and molecular weight of copolymer declines to 75 × 10^3. The increase in MA incorporation and decrease in catalytic activity are reasonable because the possibility and ratio of MA coordinated with Ni center is increased in higher MA concentration, and deactivation reaction becomes more facilitated, thus resulting in lower catalytic activity and higher MA incorporation. Furthermore, as observed, decreasing ethyele pressure has similar effect on the catalytic activity, molecular weight and MA incorporation (Table 3, entry 16 and 17).

We also perform copolymerization with longer time using catalyst **3e**. Catalyst **3e** still displays high activity (up to 21.2 × 10^3 g mol_{Ni}^{-1} h^{-1}) even reacted for two hours (entry 18, table 3). This value is only slightly decreased relative to the data of reacting for one hour (26.3 × 10^3 g mol_{Ni}^{-1} h^{-1}, entry 12, Table 3), and it is indicative of an excellent thermal stability of **3e** under 120°C.

To shed light on the influence of catalyst structure tailor on the microstructure of E–MA copolymer, [2a,2k] we also made a detailed analysis of the ^{1}H NMR spectra of copolymers produced by complexes **3c–h** (**E/MA-3c–E/MA-3h**, entry 10–15, Table 3) in presence of 0.2 mol/L MA, respectively. We find that MA units are mainly incorporated into the polymer main chain (in-chain MA) and just a few located at the chain end (terminal MA). As shown in Figure 6, ratio of terminal MA to total MA is 8.7% in both **E/MA-3c** and **E/MA-3f**, however, it is 8.0% and 8.3% in **E/MA-3d** and **E/MA-3g**, respectively. This result indicates that the percentage of terminal MA is slightly decreased by introducing an electron-withdrawing group on *ortho*-phenoxy position. That means, *β*-H elimination reaction after 2,1-insertion of MA has been slightly inhibited. In addition, terminal MA structure in **E/MA-3h** is slightly increased by 0.3% by introducing an electron-withdrawing group on the phosphorus atom relative to that in copolymer **E/MA-3e**.

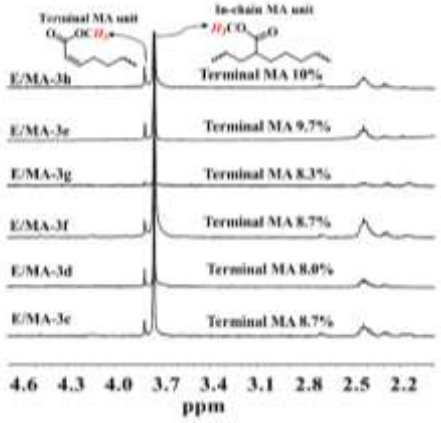

Figure 6. ^{1}H NMR spectra (expanded 4.6 to 2.2 ppm) of ethylene–methyl acrylate copolymers (**E/MA-3c–E/MA-3h**) obtained with complexes **3c**–**h** (entry 10-15, Table 3), respectively.

Table 4. Copolymerization of ethylene with challenging vinyl polar monomers by **3g.**[a)]

Entry	Comonomer (mol/L)	P (Bar)	Yield (g)	Act.[b)] (10^4)	Incorp.[c)] (mol%)	M_w[d)] (10^3)	M_w/M_n[d)]	T_m[e)] (°C)
1	$CO_2{}^nBu$ (0.2)	10	0.743	7.43	1.4	147.2	1.7	133
2	$CON(Me)_2$ (0.1)	10	0.200	2.00	0.8	39.0	1.8	132
3	$CO_2CH_2CH_2OMe$ (0.2)	10	0.095	0.95	2.2	37.9	2.5	132
4	$CO_2{}^nBu$ (0.2)	5	0.222	2.22	2.3	26.2	1.9	120
5	$CON(Me)_2$ (0.1)	5	0.061	0.61	1.2	19.6	2.2	130
6	$CO_2CH_2CH_2OMe$ (0.2)	5	0.025	0.25	3.0	11.5	2.1	119
7	$CO_2(CH_2CH_2O)_7Me$ (0.1)	10	0.635	6.35	1.0	373.6	3.1	134

Polymerization conditions: [a)] 10 μmol of catalyst, 50 mL toluene, 60 min, 50 °C . [b)] In unit of g mol_{Ni}^{-1} h^{-1}. [c)] Determined by ^{1}H NMR spectroscopy at 120 °C. [d)] Determined by GPC in 1,2,4-trichlorobenzene at 150 °C *vs* narrow polystyrene standard. [e)] Determined by DSC, the second heating curve at the rate of 20 °C min^{-1}.

Copolymerization of ethylene and various promising and challenging vinyl polar monomers. Complex **3g** bearing an electron-withdrawing substituent (6-C_6F_5) displays the highest catalytic activity in copolymerization of ethylene with MA and produces E–MA copolymer with the highest molecular weight. Herein, we further explore copolymerization of ethylene with a variety of challenging vinyl polar monomers, such as acrylamides and macromonomer, respectively. Without any cocatalyst, **3g** shows relatively high activity toward copolymerization of ethylene with butyl acrylate, *N,N*-dimethylacrylamide, or ethylene glycol

monomethyl ether acrylate with 1–3 mol% of polar comonomer incorporation. As shown in Table 4, catalytic activity for ethylene–butyl acrylate copolymerization (entry 1 and 4) was much higher than the corresponding values for acrylamide monomer (entry 2 and 5). **3g** can also effectively catalyze copolymerization of ethylene with ethyleneglycol monomethyl ether acrylate (EGMA), giving copolymer with EGMA incorporation up to 3.0 mol%. Besides, as a very important biocompatible and hydrophilic macromonomer, polyethylene glycol monomethyl ether acrylate macromonomer can also be efficiently incorporated into polyethylene main chain by using **3g** as a catalyst. As far as we know, this is the first example of direct coordination-insertion copolymerization of ethylene with these kinds of challenging vinyl functional macromonomers.

Conclusions

In conclusion, we present an excellent example to effectively improve catalytic performances by fine modification of bulky phosphino-phenolate neutral nickel catalyst structure. These modified nickel complexes are very thermally robust and exhibit high catalytic activity (up to 10^7 g·mol$_{Ni}^{-1}$·h^{-1}) even at 120 °C. Highly linear polyethylene with high molecular weight (up to 717.1 × 10^3) are obtained. Additionally, nickel complexes bearing an electron-withdrawing group or a bulky group on *ortho*-phenoxy position display increased catalytic activities toward not only ethylene polymerization but also ethylene–methyl acrylate copolymerization. More importantly, introducing an electronic-withdrawing group on *ortho*-phenoxy position contributes to enhance molecular weight at expense of MA incorporation. Conversely, nickel complex bearing an electronic-donating substituent on P-aryl moiety exhibits increased catalytic activity and produces higher molecular-weight (co)polymer toward both ethylene polymerization and copolymerization. Stoichiometric NMR experiments reveal that nickel complexes bearing an electron-withdrawing substituent on *ortho*-phenoxy position are more tolerant in the presence of excess MA. Besides, unprecedented copolymerization of ethylene and several very challenging polar vinyl monomers (such as acrylamide, ethylene glycol monomethyl ether acrylate, even polyethylene glycol monomethyl ether acrylate macromonomer) can also be efficiently achieved by the optimized Ni catalyst.

Experimental Section

General procedures and materials. All syntheses and preparations involving air/moisture-sensitive were all carried out in a glove-box (Etelux Lab 2000) under nitrogen or using standard Schlenk techniques. All solvents, such as toluene, *n*-hexane, diethyl ether, dichloromethane, were purified by Etelux solvent purification system. Dry tetrahydrofuran was purchased form *J&K* Chemicals, and used without any purification. Naphthane was distilled under reduced pressure after drying over CaH_2. Ethylene (99.9%) was purchased form BF Special Gas Limited Company and purified with a purification system (O_2 ≤ 0.1 ppm, H_2O ≤ 0.1 ppm, CO_2 ≤ 0.1 ppm). Butyl acrylate, ethyleneglycol monomethyl ether acrylate and *N,N*-dimethylacrylamide were all purchased from *J&K* Chemicals and distilled under reduced pressure after drying over CaH_2. Polyethylene glycol monomethyl ether acrylate was synthesized by the reaction of acrylic acid with polyethylene glycol monomethyl ether (M_n = 350). Compound **2e** and complex **3e** were synthesized according to our previous work.[9] NMR experiments were conducted on a Bruker spectrometer (500 MHz or 400 MHz) at 25 °C or 120 °C. The molecular weights of polyethylenes or ethylene–vinyl polar monomer copolymers were measured by gel permeation chromatography technique (1,2,4-trichlorobenzene as mobile phase) through a high-temperature chromatograph (PL-GPC 220 type) equipped with three PLgel 10 μm Mixed-B LS type columns. Melting temperatures of obtained (co)polymers were measured via a Q2000 V24.11 Build 124 differential scanning calorimeter (DSC) at a rate of 20 °C min^{-1} under N_2. Elemental analysis was performed on an elemental spectrometer (Vario EL). The X-ray analysis data of crystals were recorded on a Bruker Smart diffractometer (APEX) with CCD detector using Mo Kα radiation (λ = 0.71073Å) with the ω scan mode at 186 K. The CCDC number for complex **3b**, **3d** and **3h** is 1886371, 1886372, and 1886373, respectively. Representative NMR spectra, GPC traces, DSC traces of the polymers, and X-ray crystallography data are all provided in supporting information. This material is available free of charge via the Internet at https://onlinelibrary.wiley.com.

Syntheses of ligands. 2-(2-(2',6'-(MeO)$_2$-C$_6$H$_3$)-C$_6$H$_4$)(Ph)P-C$_6$H$_4$OH (2a). A flask was charged with 2-bromo-2',6'-dimethoxybiphenyl (3.4 g, 12 mmol) and 80 mL of dry THF, then a solution of ^{n}BuLi (14 mmol, 1.2 equivalents, 2.4 M) in hexane was slowly added via a dry syringe at 25 °C. After stirred for 3 h, reaction mixture was slowly transferred to another flask charged with a solution of $PPhCl_2$ (1.62 mL, 12 mmol) in 10 mL of THF via a glass delivery tube under N_2 atmosphere at 0 °C. Reaction temperature was slowly warmed up to room temperature. After reaction for 6 h, a clear solution **A** was formed. Meanwhile, a solution of tetrahydropyranyl (THP) ether compound C_6H_5OTHP (THP = $-C_5H_9O$, 2.14 g, 12 mmol) in diethyl ether was lithiated by 5.5 mL of ^{n}BuLi (13 mmol, 1.1 equivalents, 2.4 M in hexane) and stirred for 4 h at room temperature, yielding suspension **B**. The formed suspension **B** was slowly transferred to reaction mixture **A** via a glass delivery tube at 0 °C. After reaction for 8 h at room temperature, all solvents were removed under vacuum, and the obtained residue 2-(2-(2',6'-(MeO)$_2$-C$_6$H$_3$)-C$_6$H$_4$)(Ph)P-C$_6$H$_4$OTHP (**1a**) was used in next reaction step without purification. The residue was dissolved in degassed ethyl acetate, and a few drops of hydrochloric acid was added. After stirred for 3 h, the protected group was completely removed by TLC monitoring. Resultant mixture was quenched by aqueous $NaHCO_3$ and extracted with ethyl acetate. Organic phase was dried by anhydrous magnesium sulfate, and pure target compound **2a** was obtained by column chromatography (petroleum ether/ethyl acetate = 30/1) as white solids (2.5 g, 51 wt%). ^{1}H NMR (400 MHz, C_6D_6): δ 7.52–7.44 (m, 1H), 7.38–7.27 (m, 3H), 7.14–7.09 (m, 2H), 7.08–6.94 (m, 6H), 6.69 (td, *J* = 7.3, 1.2 Hz, 1H), 6.60 (d, *J* = 7.7 Hz, 1H), 6.32 (dd, *J* = 23.3, 8.3 Hz, 2H), 3.22 (s, –OC*H*$_3$, 3H), 3.09 (s, –OC*H*$_3$, 3H). ^{1}H NMR (400 MHz, DMSO-*d*$_6$): δ 9.46 (s, –O*H*, 1H), 7.38–7.18 (m, 6H), 7.17–7.01 (m, 4H), 6.95–6.90 (m, 1H), 6.78–6.66 (m, 2H), 6.62–6.56 (m, 2H), 6.53 (m, 1H), 3.47 (s, –OC*H*$_3$, 3H), 3.36 (s, –OC*H*$_3$, 3H).^{13}C NMR (101 MHz, C_6D_6): δ 142.5, 142.2, 135.6, 134.1, 133.9, 133.7, 133.5, 131.4 (d, *J* = 6.6 Hz), 130.8, 129.5, 129.3, 122.6, 120.5, 119.5, 115.6, 104.0, 103.9 (d, *J* = 13.0 Hz), 103.98, 55.4 (–O*C*H$_3$), 55.2 (–O*C*H$_3$). ^{31}P NMR

(162 MHz, C_6D_6): δ -35.99. Anal. calcd. for $C_{26}H_{23}O_3P$: C, 75.35; H, 5.59. Found: C, 75.41; H, 5.64.

2-(2-(2',6'-(MeO)$_2$-C$_6$H$_3$)-C$_6$H$_4$)(Ph)P-6-F-C$_6$H$_3$OH (2b). Following a procedure similar to that for ligand **2a**, using 2-F-C_6H_4OTHP instead of C_6H_5OTHP, ligand **2b** was obtained in yield of 57 wt%. ^{1}H NMR (400 MHz, C_6D_6): δ 7.44–7.39 (m, 1H), 7.37–7.32 (m, 1H), 7.28 (m, 2H), 7.10 (t, *J* = 8.3 Hz, 1H), 7.00 (m, 4H), 6.80 (dd, *J* = 9.5, 1.4 Hz, 2H), 6.43 (td, *J* = 8.0, 4.6 Hz, 1H), 6.35-6.32 (m, 2H), 6.28 (d, *J* = 8.3 Hz, 1H), 3.23 (s, –OC*H*$_3$, 3H), 3.06 (s, –OC*H*$_3$, 3H).^{1}H NMR (400 MHz, DMSO-*d*$_6$): δ 9.65 (s, –O*H*, 1H), 7.38–7.28 (m, 4H), 7.24 (t, *J* = 8.3 Hz, 2H), 7.17–7.01 (m, 4H), 6.91 (ddd, *J* = 7.7, 3.6, 1.4 Hz, 1H), 6.72 (tdd, *J* = 8.0, 4.8, 1.0 Hz, 1H), 6.59 (dd, *J* = 8.3, 4.9 Hz, 2H), 6.33 (dd, *J* = 7.5, 3.9 Hz, 1H), 3.47 (s, –OC*H*$_3$, 3H), 3.38 (s, –OC*H*$_3$, 3H). ^{13}C NMR (101 MHz, C_6D_6): δ 158.45, 158.15, 152.77, 150.37, 147.45 (dd, *J* = 20.0, 11.2 Hz), 142.86, 142.51, 135.70 (dd, *J* = 16.9, 6.9 Hz), 134.64–133.42 (m), 131.83 (d, *J* = 6.5 Hz), 129.88, 129.63, 129.09, 126.75 (d, *J* = 12.3 Hz), 120.40 (d, *J* = 5.7 Hz), 119.74 (d, *J* = 8.0 Hz), 117.00 (d, *J* = 18.1 Hz), 104.35 (d, *J* = 4.6 Hz), 55.50(–OCH$_3$), 55.12(–OCH$_3$). ^{31}P NMR (162 MHz, C_6D_6): δ -33.23 (d, *J* = 8.7 Hz). ^{19}F NMR (376 MHz, C_6D_6): δ -136.77 (d, *J* = 8.7 Hz). Anal. calcd. for $C_{26}H_{22}FO_3P$: C, 72.22; H, 5.13. Found: C, 72.03; H, 5.20.

2-(2-(2',6'-(MeO)$_2$-C$_6$H$_3$)-C$_6$H$_4$)(Ph)P-6-CH$_3$-C$_6$H$_3$OH (2c). Following a procedure similar to that for ligand **2a**, using 2-CH_3-C_6H_4OTHP instead of C_6H_5OTHP, ligand **2c** was obtained in yield of 45 wt%. ^{1}H NMR (400 MHz, C_6D_6): δ 7.51 (ddd, *J* = 7.7, 4.2, 1.0 Hz, 1H), 7.37–7.27 (m, 3H), 7.11 (t, *J* = 8.3 Hz, 1H), 7.07–7.02 (m, 1H), 7.01–6.94 (m, 5H), 6.77 (d, *J* = 8.7 Hz, 1H), 6.69 (t, *J* = 7.5 Hz, 1H), 6.31 (dd, *J* = 26.2, 8.3 Hz, 2H), 3.23 (s, –OC*H*$_3$, 3H), 3.06 (s, –OC*H*$_3$, 3H), 2.28 (s, 3H, –C*H*$_3$). ^{1}H NMR (400 MHz, DMSO-*d*$_6$): δ 8.33 (s, –O*H*, 1H), 7.42–7.18 (m, 6H), 7.07 (dddd, *J* = 15.9, 7.2, 4.8, 1.8 Hz, 4H), 6.92 (ddd, *J* = 7.7, 3.5, 1.4 Hz, 1H), 6.66 (t, *J* = 7.5 Hz, 1H), 6.58 (dd, *J* = 8.3, 2.2 Hz, 2H), 6.38 (ddd, *J* = 7.8, 4.1, 1.7 Hz, 1H), 3.45 (s, –OC*H*$_3$, 3H), 3.40 (s, –OC*H*$_3$, 3H), 2.13 (s, –C*H*$_3$, 3H).^{13}C NMR (101 MHz, C_6D_6): δ 158.47, 158.16, 158.14, 157.96, 142.71, 142.37, 136.19, 136.12, 136.00 (d, *J* = 2.5 Hz), 134.10 (d, *J* = 1.7 Hz), 134.04, 133.85, 132.48, 132.18 (d, *J* = 2.1 Hz), 131.70 (d, *J* = 6.6 Hz), 129.74, 129.57, 128.47, 128.41, 128.00, 124.59 (d, *J* = 1.5 Hz), 121.97 (d, *J* = 6.0 Hz), 120.56 (d, *J* = 1.6 Hz), 119.70 (d, *J* = 8.0 Hz), 104.25, 104.09, 55.34 (–OCH$_3$), 55.10 (–OCH$_3$), 16.54 (d, *J* = 2.7 Hz, –CH$_3$). ^{31}P NMR (162 MHz, C_6D_6): δ -36.61. Anal. calcd. for $C_{27}H_{25}O_3P$: C, 75.69; H, 5.88. Found: C, 75.55; H, 5.84.

2-(2-(2',6'-(MeO)$_2$-C$_6$H$_3$)-C$_6$H$_4$)(Ph)P-6-CF$_3$-C$_6$H$_3$OH (2d). Following a procedure similar to that for ligand **2a**, using 2-CF_3-C_6H_4OTHP instead of C_6H_5OTHP, ligand **2d** was obtained in yield of 42 wt%. ^{1}H NMR (400 MHz, C_6D_6): δ 7.40–7.27 (m, 3H), 7.25 (d, *J* = 7.9 Hz, 1H), 7.22–7.11 (m, 3H), 7.09 (t, *J* = 8.4 Hz, 1H), 7.00–6.93 (m, 4H), 6.45 (t, *J* = 7.7 Hz, 1H), 6.28 (dd, *J* = 18.3, 8.3 Hz, 2H), 3.15 (s, –OC*H*$_3$, 3H), 3.06 (s, –OC*H*$_3$, 3H). ^{1}H NMR (400 MHz, DMSO-*d*$_6$): δ 9.24 (s, –O*H*, 1H), 7.52 (dd, *J* = 7.9, 1.7 Hz, 1H), 7.45–7.21 (m, 6H), 7.10 (dddd, *J* = 23.8, 7.2, 4.6, 2.4 Hz, 3H), 7.03–6.89 (m, 3H), 6.64 (d, *J* = 8.4 Hz, 1H), 6.55 (d, *J* = 8.4 Hz, 1H), 3.56 (s, –OC*H*$_3$, 3H), 3.28 (s, –OC*H*$_3$, 3H).^{13}C NMR (101 MHz, C_6D_6): δ 158.27 (d, *J* = 0.8 Hz), 157.94 (d, *J* = 1.1 Hz), 157.78 (d, *J* = 1.6 Hz), 157.56 (d, *J* = 1.6 Hz), 142.76, 142.42, 138.16, 134.85 (d, *J* = 1.1 Hz), 134.77, 134.70, 133.87, 133.72 (d, *J* = 1.7 Hz), 133.69, 131.89 (d, *J* = 6.8 Hz), 130.17, 129.88, 128.71, 128.64, 128.42, 126.04 (d, *J* = 2.7 Hz), 125.49, 125.39, 123.33 (d, *J* = 2.7 Hz), 120.06, 119.25 (d, *J* = 8.2 Hz), 117.20 (qd, *J* = 31.1, 2.0 Hz, –CF$_3$), 104.29 (d, *J* = 9.8 Hz), 55.39 (–OCH$_3$), 55.16 (–OCH$_3$). ^{31}P NMR (162 MHz, C_6D_6): δ -38.57. ^{19}F NMR (376 MHz, C_6D_6): δ -61.93. Anal. calcd. for $C_{27}H_{22}F_3O_3P$: C, 67.22; H, 4.60. Found: C, 67.27; H, 4.52.

2-(2-(2',6'-(MeO)$_2$-C$_6$H$_3$)-C$_6$H$_4$)(Ph)P-6-Ph-C$_6$H$_3$OH (2f). Following a procedure similar to that for ligand **2a**, using 2-Ph-C_6H_4OTHP instead of C_6H_5OTHP, ligand **2f** was obtained in yield of 53 wt%. ^{1}H NMR (400 MHz, C_6D_6): δ 7.65–7.59 (m, 2H), 7.54 (dd, *J* = 8.2, 4.7 Hz, 1H), 7.41–7.31 (m, 3H), 7.29–7.10 (m, 10H), 6.78 (t, *J* = 7.5 Hz, 2H), 6.30 (dd, *J* = 10.3, 8.4 Hz, 2H), 3.16 (s, –OC*H*$_3$, 3H), 3.09 (s, –OC*H*$_3$, 3H). ^{1}H NMR (400 MHz, DMSO-*d*$_6$): δ 8.28 (s, –O*H*, 1H), 7.47–7.21 (m, 12H), 7.17 (dt, *J* = 7.4, 1.3 Hz, 1H), 7.15–7.08 (m, 3H), 6.98 (dd, *J* = 7.6, 2.6 Hz, 1H), 6.87 (t, *J* = 7.6 Hz, 1H), 6.65–6.55 (m, 3H), 3.50 (s, –OC*H*$_3$, 3H), 3.39 (s, –OC*H*$_3$, 3H). ^{13}C NMR (101 MHz, C_6D_6): δ 158.39, 158.19, 156.72, 156.52, 142.66, 142.33, 139.04 (d, *J* = 3.62), 136.14, 136.06, 136.03, 134.11–133.92(m), 132.44, 131.78 (d, *J* = 6.5 Hz), 129.98, 129.66 (d, *J* = 9.5 Hz, 5H), 128.91, 127.15, 123.70, 104.13 (d, *J* = 9.0 Hz), 55.30 (–OCH$_3$), 55.09 (–OCH$_3$). ^{31}P NMR (162 MHz, C_6D_6): δ -35.52. Anal. calcd. for $C_{32}H_{27}O_3P$: C, 78.35; H, 5.55. Found: C, 78.25; H, 5.48.

2-(2-(2',6'-(MeO)$_2$-C$_6$H$_3$)-C$_6$H$_4$)(Ph)P-6-C$_6$F$_5$-C$_6$H$_3$OH (2g). A flask was charged with complex **1a** (1.8 g, 3.6 mmol) and 20 mL of dry THF, cooled to 0 °C and a solution of ^{n}BuLi in hexane (2.4 M, 1.5 mL, 1.2 equivalents) was added dropwise. The formed suspension was cooled to -50 °C, followed by slow addition of hexafluorobenzene (3.3 g, 18 mmol, 5 equivalents). After reaction overnight, volatiles was removed by a rotary evaporator, and the obtained residue was dissolved in degassed ethyl acetate. Few drops of hydrochloric acid was added slowly. After stirring for 5 h, the protected group was completely removed monitoring by TLC. Resultant mixture was quenched by aqueous $NaHCO_3$, and then extracted with ethyl acetate. Organic phase was dried in anhydrous magnesium sulfate, and concentrated by a rotary evaporator. Pure target compound **2g** was obtained by column chromatography (petroleum ether/ethyl acetate = 15/1) as white solids (1.5 g, 75 wt%). ^{1}H NMR (400 MHz, C_6D_6): δ 7.45 (ddd, *J* = 7.6, 4.2, 1.0 Hz, 1H), 7.35–7.24 (m, 3H), 7.23–7.13 (m, 4H), 7.23–7.06 (m, 5H), 7.10 (t, *J* = 8.4 Hz, 1H), 7.06–6.95 (m, 5H), 6.92 (d, *J* = 7.9 Hz, 1H), 6.92 (d, *J* = 7.9 Hz, 1H), 6.73 (t, *J* = 7.6 Hz, 1H), 6.73 (t, *J* = 7.6 Hz, 1H), 6.35 (d, *J* = 8.3 Hz, 1H), 6.27 (d, *J* = 8.3 Hz, 1H), 3.19 (s,–OC*H*$_3$, 3H), 3.06 (s, –OC*H*$_3$, 3H). ^{1}H NMR (400 MHz, DMSO-*d*$_6$): δ 8.98 (s, –O*H*, 1H), 7.42–7.18 (m, 7H), 7.10 (m, 3H), 6.97 (dd, *J* = 8.0, 3.4 Hz, 1H), 6.92 (t, *J* = 7.6 Hz, 1H), 6.72–6.64 (m, 1H), 6.60 (d, *J* = 8.4 Hz, 2H), 3.45 (s, –OC*H*$_3$, 3H), 3.38 (s, –OC*H*$_3$, 3H).^{13}C NMR (101 MHz, C_6D_6): δ 158.37, 158.02, 157.37, 157.16, 146.06, 142.78, 142.45, 136.12, 135.09, 135.02, 134.05, 133.87, 133.04, 131.87 (d, *J* = 6.6 Hz), 130.14, 129.77, 128.72, 128.65, 124.47 (d, *J* = 9.3 Hz), 120.74, 119.45 (d, *J* = 8.1 Hz), 113.71, 104.31 (d, *J* = 11.3 Hz), 55.39 (–OCH$_3$), 55.15 (–OCH$_3$). ^{31}P NMR (162 MHz, C_6D_6): δ -36.13. ^{19}F NMR (376 MHz, C_6D_6): δ -140.36 (ddd, *J* = 100.8, 23.8, 8.0 Hz), -156.46 (t, *J* = 21.5 Hz), -163.35 – -163.72 (m). Anal. calcd. for $C_{32}H_{22}F_5O_3P$: C, 66.21; H, 3.82. Found: C, 66.11; H, 3.74.

2-(2-(2',6'-F$_2$-C$_6$H$_3$)-C$_6$H$_4$)(Ph)P-6-^{t}Bu-C$_6$H$_3$OH (2h). The synthetic procedure was similar to that for ligand **2a**, except using 2-^{t}Bu-C_6H_4OTHP instead of C_6H_5OTHP. Note that the reaction of 2-bromo-2',6'-difluorobiphenyl (2.7 g, 10 mmol) with ^{n}Buli was carried out at -78 °C. **2h** was obtained as withe solids in yield of

63 wt%. ^{1}H NMR (400 MHz, C_6D_6): δ 7.37–7.32 (m, 1H), 7.28–7.24 (m, 3H), 7.12–7.06 (m, 1H), 7.06–7.00 (m, 2H), 6.99–6.92 (m, 5H), 6.73 (t, *J* = 7.6 Hz, 1H), 6.70–6.63 (m, 1H), 6.52 (td, *J* = 8.4, 5.3 Hz, 2H), 1.45 (s, –C(C*H*$_3$)$_3$, 9H).^{13}C NMR (101 MHz, C_6D_6): δ 162.04 (d, *J* = 7.0 Hz), 161.59 (d, *J* = 7.1 Hz), 159.61, 159.16, 159.09, 159.05, 158.83, 137.26 (d, *J* = 3.8 Hz), 136.15, 135.60, 135.30, 134.46 (d, *J* = 1.8 Hz), 133.88, 133.66 (d, *J* = 7.8 Hz), 133.39, 131.37 (d, *J* = 5.7 Hz), 130.14 (t, *J* = 10.0 Hz), 129.47 (d, *J* = 4.8 Hz), 129.20 , 129.05–128.73 (m), 120.93 (d, *J* = 1.7 Hz), 120.44 , 118.62 (dd, *J* = 21.1, 7.5 Hz), 111.59 (d, *J* = 3.4 Hz), 111.50–111.30 (m), 111.20 (d, *J* = 3.5 Hz), 35.14 (d, *J* = 1.9 Hz, –*C*(CH$_3$)$_3$), 29.83 (–C(*C*H$_3$)$_3$). ^{31}P NMR (162 MHz, C_6D_6): δ -39.06 (t, *J* = 24.4 Hz). ^{19}F NMR (376 MHz, C_6D_6): δ -110.38 (dd, *J* = 24.5, 4.8 Hz), -110.54 (dd, *J* = 24.5, 4.8 Hz). Anal. calcd. for $C_{28}H_{25}F_2OP$: C, 75.32; H, 5.64. Found: C, 75.38; H, 5.74.

General procedure for synthesis of nickel complexes. In a 50-mL flask, Py_2NiMe_2 (0.15 g, 0.6 mmol, 1.2 equivalents) was dissolved in 10 mL of dry toluene, a solution of respective phosphino-phenolate ligand **2a**-**h** in 15 mL of dry toluene was slowly added under vigorous stirring at room temperature. After reaction for 6 h, a black suspension was yielded. The suspension was filtered to remove the black nickel. The red-brown filtrate was concentrated to give crude product. Pure complex was obtained by recrystallization from toluene/hexane.

[2-(2-(2',6'-(MeO)$_2$-C$_6$H$_3$)-C$_6$H$_4$)(Ph)P-C$_6$H$_4$O] Ni(Me)(Py) (3a). Following the general procedure, complex **3a** was prepared from the reaction of Py_2NiMe_2 (0.15 g, 0.6 mmol, 1.2 equivalents) with ligand **2a** (0.21 g, 0.5 mmol) as a yellow solid (0.23 g, 80 wt%). ^{1}H NMR (400 MHz, C_6D_6): δ 8.43 (s, 2H), 7.78–7.60 (m, 3H), 7.49–7.46 (m, 1H), 7.37–7.32 (m, 1H), 7.08–6.96 (m, 8H), 6.62 (d, *J* = 8.3 Hz, 1H), 6.55 (t, *J* = 7.3 Hz, 1H), 6.47–6.44 (m, 2H), 6.39 (d, *J* = 8.3 Hz, 1H), 3.39 (s, 3H, –OC*H*$_3$), 3.13 (s, 3H, –OC*H*$_3$), -0.78 (d, *J* = 5.0 Hz, 3H, Ni–C*H*$_3$). ^{13}C NMR (101 MHz, C_6D_6): δ 177.08, 159.81, 158.45, 141.81, 134.69, 133.47 (d, *J* = 9.2 Hz), 133.24 (d, *J* = 10.5 Hz), 132.74, 132.65, 132.07, 131.29, 130.77, 130.06, 126.74 (d, *J* = 6.6 Hz), 118.82 (d, *J* = 9.5 Hz), 113.53, 103.46, 103.18, 54.97 (–O*C*H$_3$), 54.56(–O*C*H$_3$), -14.00 (d, *J* = 36.8 Hz, Ni–*C*H$_3$). ^{31}P NMR (162 MHz, C_6D_6): δ 21.09. Anal. calcd. for $C_{32}H_{30}NNiO_3P$: C, 67.88; H, 5.34; N, 2.47. Found: C, 67.74; H, 5.44; N, 2.35.

[6-F-2-(2-(2',6'-(MeO)$_2$-C$_6$H$_3$)-C$_6$H$_4$)(Ph)P-C$_6$H$_3$O]Ni(Me)(Py) (3b). Following the general procedure, complex **3b** was prepared from the reaction of Py_2NiMe_2 (0.15 g, 0.6 mmol, 1.2 equivalents) with ligand **2b** (0.21 g, 0.5 mmol) as a yellow solid (0.22 g, 75 wt%). ^{1}H NMR (500 MHz, C_6D_6): δ 8.45 (d, *J* = 4.1 Hz, 2H), 7.74–7.55 (m, 3H), 7.44 (dd, *J* = 7.2, 4.5 Hz, 1H), 7.28–7.17 (m, 1H), 7.12–6.88 (m, 7H), 6.74 (t, *J* = 7.0 Hz, 1H), 6.58 (d, *J* = 8.3 Hz, 1H), 6.52–6.39 (m, 2H), 6.37 (d, *J* = 8.3 Hz, 1H), 6.35–6.25 (m, 1H), 3.38 (s, 1H, –OC*H*$_3$), 3.15 (s, 1H, –OC*H*$_3$), -0.78 (d, *J* = 5.1 Hz, 3H, Ni–C*H*$_3$). ^{13}C NMR (101 MHz, C_6D_6): δ 159.66, 158.38, 150.58, 141.82 (d, *J* = 22.5 Hz), 136.35, 135.93–135.64 (m), 134.43, 133.51 (d, *J* = 8.5 Hz), 132.71 (d, *J* = 9.5 Hz), 132.07, 130.22, 129.45, 129.08, 127.19–126.49 (m), 124.77, 124.28, 123.34, 119.98, 117.39 (d, *J* = 18.0 Hz), 112.58, 103.60, 103.19, 54.98 (–O*C*H$_3$), 54.39 (–O*C*H$_3$), -13.90 (d, *J* = 37.5 Hz, Ni–*C*H$_3$). ^{31}P NMR (162 MHz, C_6D_6): δ 20.80 (d, *J* = 12.6 Hz). ^{19}F NMR (376 MHz, C_6D_6): δ -137.77 (d, *J* = 12.4 Hz). Anal. calcd. for $C_{32}H_{29}FNNiO_3P$: C, 65.79; H, 5.00; N, 2.40. Found: C, 65.63; H, 5.07; N, 2.32.

[6-CH$_3$-2-(2-(2',6'-(MeO)$_2$-C$_6$H$_3$)-C$_6$H$_4$)(Ph)P-C$_6$H$_3$O]Ni(Me)(Py) (3c). Following the general procedure, complex **3c** was prepared from the reaction of Py_2NiMe_2 (0.12 g, 0.5 mmol, 1.2 equivalents) with ligand **2c** (0.17 g, 0.4 mmol) as a yellow solid (0.21 g, 89 wt%). ^{1}H NMR (400 MHz, C_6D_6): δ 8.46 (d, *J* = 4.0 Hz, 2H), 7.69 (dt, *J* = 12.3, 8.5 Hz, 3H), 7.47 (dd, *J* = 7.0, 4.5 Hz, 1H), 7.27 (t, *J* = 8.4 Hz, 1H), 7.24-7.29 (m, 1H), 7.17-7.12 (m, 3H), 7.03–6.93 (m, 8H (5H, toluene, 3H, Ar-*H*)), 6.81 (t, *J* = 6.6 Hz, 1H), 6.66–6.45 (m, 4H), 6.37 (d, *J* = 8.3 Hz, 1H), 3.39 (s, 3H, –OC*H*$_3$), 3.03 (s, 3H, –OC*H*$_3$), 2.37 (d, *J* = 14.4 Hz, 3H), -0.87 (dd, *J* = 65.8, 4.2 Hz, 3H, Ni–C*H*$_3$). ^{13}C NMR (101 MHz, C_6D_6): δ 175.5, 175.3 159.7, 158.4, 150.6, 141.7, 141.57, 137.9, 137.3, 136. 8, 136.1, 134.6, 133.4 (d, *J* = 9.2 Hz), 133.2, 132.8 (d, *J* = 9.5 Hz), 132. 6, 130.0 (d, *J* = 2.0 Hz), 129.7 (d, *J* = 1.1 Hz), 129.3, 129.2, 128.8 (d, *J* = 2.1 Hz), 126.7 (d, *J* = 6.6 Hz), 126.37 (d, *J* = 9.6 Hz), 125.7, 123.1, 120.2 (d, *J* = 5.1 Hz), 119.3, 118.8, 113.5 (d, *J* = 7.5 Hz), 103.2 (d, *J* = 23.0 Hz), 54.95(–O*C*H$_3$), 54.17 (–O*C*H$_3$), 17.5 (–*C*H$_3$), -13.9 (d, *J* = 37.1 Hz, Ni–*C*H$_3$). ^{31}P NMR (162 MHz, C_6D_6): δ 21.27. Anal. calcd. for $C_{33}H_{32}NNiO_3P$: C, 68.30; H, 5.56; N, 2.41. Found: C, 68.22; H, 5.43; N, 2.34.

[6-CF$_3$-2-(2-(2',6'-(MeO)$_2$-C$_6$H$_3$)-C$_6$H$_4$)(Ph)P-C$_6$H$_3$O]Ni(Me)(Py) (3d). Following the general procedure, complex **3d** was prepared from the reaction of Py_2NiMe_2 (0.12 g, 0.5 mmol, 1.2 equivalents) with ligand **2d** (0.19 g, 0.4 mmol) as a brown solid (0.22 g, 86 wt%). ^{1}H NMR (400 MHz, C_6D_6): δ 8.41 (s, broad, 2H), 7.66–7.50 (m, 4H), 7.43 (dd, *J* = 6.7, 4.5 Hz, 1H), 7.32 (t, *J* = 8.3 Hz, 1H), 7.22–7.18 (m, 1H), 7.12 (t, *J* = 3.7 Hz, 1H), 7.08–6.91 (m, 5H), 6.83–6.72 (m, 1H), 6.50 (d, *J* = 8.3 Hz, 3H), 6.31 (dd, *J* = 12.6, 7.8 Hz, 2H), 3.36 (s, 3H, –OC*H*$_3$), 3.08 (s, 1H, –OC*H*$_3$), -0.77 (d, *J* = 5.1 Hz, 3H, Ni–C*H*$_3$). ^{13}C NMR (101 MHz, C_6D_6): δ 159.46, 158.25, 150.51, 141.91 (d, *J* = 17.2 Hz), 136.51, 136.07, 135.94, 135.44, 134.45, 133.61 (d, *J* = 9.3 Hz), 132.67 (d, *J* = 9.6 Hz), 132.03, 131.52, 130.35 (d, *J* = 2.0 Hz), 130.06 (d, *J* = 4.8 Hz), 129.57, 129.34, 129.18 (d, *J* = 1.8 Hz), 128.58 (d, *J* = 2.5 Hz), 128.50, 126.80 (d, *J* = 6.8 Hz), 125.70, 125.20, 124.71, 123.22, 119.65 (d, *J* = 5.3 Hz), 119.65 (d, *J* = 5.3 Hz), 112.07 (d, *J* = 6.9 Hz), 103.52, 103.25, 54.96 (–O*C*H$_3$), 54.46 (–O*C*H$_3$), -14.07 (d, *J* = 37.6 Hz, Ni–*C*H$_3$). ^{31}P NMR (162 MHz, C_6D_6): δ 19.92. ^{19}F NMR (376 MHz, C_6D_6): δ -62.39. Anal. calcd. for $C_{33}H_{29}F_3NNiO_3P$: C, 62.49; H, 4.61; N, 2.21. Found: C, 62.43; H, 4.56; N, 2.18.

[6-Ph-2-(2-(2',6'-(MeO)$_2$-C$_6$H$_3$)-C$_6$H$_4$)(Ph)P-C$_6$H$_3$O]Ni(Me)(Py) (3f). Following the general procedure, complex **3f** was prepared from the reaction of Py_2NiMe_2 (0.12 g, 0.5 mmol, 1.2 equivalents) with ligand **2f** (0.20 g, 0.4 mmol) as a yellow solid (0.23 g, 90 wt %). ^{1}H NMR (400 MHz, C_6D_6): δ 8.38 (dd, *J* = 4.9, 1.6 Hz, 2H), 7.97–7.93 (m, 2H), 7.68 (m, 3H), 7.50–7.43 (m, 2H), 7.32–7.26 (m, 3H), 7.20 (d, *J* = 7.4 Hz, 2H), 7.14–6.95 (m, 10H), 6.83 (t, *J* = 7.6 Hz, 1H), 6.62 (td, *J* = 7.4, 1.9 Hz, 1H), 6.56–6.46 (m, 2H), 6.34 (d, *J* = 9.0 Hz, 2H), 3.38 (s, 3H, –OC*H*$_3$), 3.01 (s, 3H, –OC*H*$_3$), -0.75 (d, *J* = 5.0 Hz, 3H, Ni–C*H*$_3$). ^{13}C NMR (101 MHz, C_6D_6): δ 173.7 (d, *J* = 21.2 Hz), 159.7, 158.3, 150.8, 141.9, 141.7, 136.7, 136.3, 134.5, 133.5 (d, *J* = 9.3 Hz), 132.8, 132.7, 132.5 (d, *J* = 5.2 Hz), 131.9, 130.1, 129.7, 129.6, 129.3, 129.0, 126.8 (d, *J* = 6.5 Hz), 125.8, 125.7, 123.0, 122.4, 121. 9, 120.0 (d, *J* = 5.2 Hz), 114.2 (d, *J* = 7.4 Hz), 103.4, 103.1, 54.9 (–O*C*H$_3$), 54.6 (–O*C*H$_3$), -14.1 (d, *J* = 36.8 Hz, Ni–*C*H$_3$). ^{31}P NMR (162 MHz, C_6D_6): δ 21.28. Anal. calcd. for $C_{38}H_{34}NNiO_3P$: C, 71.05; H, 5.34; N, 2.18. Found: C, 71.97; H, 5.26; N, 2.04.

[6-C$_6$F$_5$-2-(2-(2',6'-(MeO)$_2$-C$_6$H$_3$)-C$_6$H$_4$)(Ph)P-C$_6$H$_3$O]Ni(Me)(Py) (3g). Following the general procedure, complex **3g** was prepared

from the reaction of Py_2NiMe_2 (0.12 g, 0.5 mmol, 1.2 equivalents) with ligand **2g** (0.23 g, 0.4 mmol) as a reddish brown solid (0.26 g, 90 wt%). ^{1}H NMR (500 MHz, C_6D_6): δ 8.31–8.20 (m, 2H), 7.64–7.55 (m, 3H), 7.45 (ddd, *J* = 7.7, 4.5, 1.1 Hz, 1H), 7.35 (ddd, *J* = 9.4, 7.6, 1.7 Hz, 1H), 7.24–7.16 (m, 2H), 7.16–7.13 (m, 1H), 7.05–6.92 (m, 4H), 6.74 (t, *J* = 7.6 Hz, 1H), 6.59–6.45 (m, 4H), 6.34 (d, *J* = 8.0 Hz, 1H), 3.34 (s, 3H, –OCH_3), 3.09 (s, 3H, –OCH_3), -0.79 (d, *J* = 5.2 Hz, 3H, Ni–CH_3). ^{13}C NMR (101 MHz, C_6D_6): δ 173.43 (d, *J* = 21.3 Hz), 159.60, 158.33, 150.45, 141.87, 136.47, 134.80, 134.36, 134.13, 133.59 (d, *J* = 9.6 Hz), 132.44 (d, *J* = 9.6 Hz), 131.89, 130.37, 129.49, 129.11, 126.80 (d, *J* = 6.0 Hz), 123.10, 122.87, 122.39, 119.79 (d, *J* = 5.3 Hz), 115.18 (d, *J* = 10.5 Hz), 113.23 (d, *J* = 7.6 Hz), 103.37 (d, *J* = 31.0 Hz), 54.95 (–OCH_3), 54.12 (–OCH_3), -14.31 (d, *J* = 36.5 Hz, Ni–CH_3). ^{31}P NMR (162 MHz, C_6D_6): δ 20.39. ^{19}F NMR (376 MHz, C_6D_6): δ -137.89 (dd, *J* = 24.3, 7.7 Hz), -140.07 (dd, *J* = 24.5, 7.7 Hz), -159.95 (t, *J* = 21.4 Hz), -164.23–-166.63 (m). Anal. calcd. for $C_{38}H_{29}F_5NNiO_3P$: C, 62.33; H, 3.99; N, 1.91. Found: C, 62.24; H, 4.03; N, 1.83.

[6-^{t}Bu-2-(2-(2',6'-F_2-C_6H_3)-C_6H_4)PhP-C_6H_3O]Ni(Me)(Py) (3h). Following the general procedure, complex **3h** was prepared from the reaction of Py_2NiMe_2 (0.12 g, 0.5 mmol, 1.2 equivalents) with ligand **2h** (0.18 g, 0.4 mmol) as a yellowish brown solid (0.21 g, 90 wt%). ^{1}H NMR (400 MHz, C_6D_6): δ 8.45 (d, *J* = 5.2 Hz, 2H), 7.82 (ddt, *J* = 10.1, 6.8, 1.6 Hz, 2H), 7.55 (t, *J* = 8.6 Hz, 1H), 7.32 (d, *J* = 7.2 Hz, 1H), 7.18–7.14 (m, 2), 7.11–7.00 (m, 4H), 6.94 (t, *J* = 7.6 Hz, 1H), 6.84–6.76 (m, 2H), 6.69 (dt, *J* = 16.8, 8.2 Hz, 2H), 6.59 (td, *J* = 7.4, 2.2 Hz, 1H), 6.52–6.44 (m, 2H), 1.54 (s, 9H), –0.53 (dd, *J* = 4.9, 2.8 Hz, 3H). ^{13}C NMR (101 MHz, C_6D_6): δ 175.23 (d, *J* = 21.1 Hz), 163.14 (d, *J* = 6.9 Hz), 162.06 (d, *J* = 6.7 Hz), 160.65 (d, *J* = 7.3 Hz), 159.60 (d, *J* = 6.9 Hz), 150.65, 137.88 (d, *J* = 9.2 Hz), 136.48, 135.29 (d, *J* = 15.5 Hz), 134.60, 134.48, 134.33 (d, *J* = 2.7 Hz), 134.13, 133.98, 133.43, 133.33, 132.62 (d, *J* = 8.3 Hz), 130.75, 130.09, 129.77, 129.68, 129.58, 129.47, 128.72, 128.63, 128.21, 127.94, 123.17, 119.17, 118.66, 113.92 (d, *J* = 7.8 Hz), 111.77 (dd, *J* = 22.2, 3.4 Hz), 111.13 (dd, *J* = 22.1, 3.3 Hz), 35.16 (–*C*$(CH_3)_3$), 29.81 (–C$(CH_3)_3$), -13.50 (dd, *J* = 36.3, 3.4 Hz, Ni–CH_3). ^{31}P NMR (162 MHz, C_6D_6): δ 24.68. ^{19}F NMR (376 MHz, C_6D_6): δ -110.12 (dd, *J* = 26.6, 5.4 Hz), -110.51 (dd, *J* = 22.1, 5.2 Hz). Anal. calcd. for $C_{34}H_{31}F_2NNiOP$: C, 68.37; H, 5.23. Found: C, 68.25; H, 5.14.

Synthesis of polyethylene glycol monomethyl ether acrylate macromonomer. A 100 mL vial was charged with acrylic acid (11.9 g, 0.165 mmol), polyethylene glycol monomethyl ether (M_n = 350, 21 g, 0.600 mmol) and hydroquinone (0.32 g, 0.003 mmol). The reaction system was heated up to 80 °C, *p*-toluenesulfonic acid (0.34 g, 1 wt%) as catalyst was added. After reacted for 7 h at 130 °C, reaction mixture was disolved in dichloromethane, washed with sodium hydroxide dilute solution two times, and then washed with water three times. Organic layer was collected, dried in anhydrous sodium sulfate and concentrated by a rotary evaporator. Pure target macromonomer was obtained by column chromatography (petroleum ether/ethyl acetate = 1/1) as colorless liquid (15 g, 51 wt%). ^{1}H NMR (400 MHz, $CDCl_3$): δ 6.43 (dd, *J* = 17.3, 1.5 Hz, 1H), 6.16 (dd, *J* = 17.3, 10.4 Hz, 1H), 5.84 (dd, *J* = 10.4, 1.4 Hz, 1H), 4.36–4.28 (m, 2H), 3.80–3.71 (m, 2H), 3.66–3.63 (m, 18H), 3.54–3.56 (m, 2H), 3.38 (s, –OCH_3, 3H).

Ethylene Polymerization Procedure. A steel autoclave (200 mL) was maintained at required reaction temperature after heating for 6 h at 150 °C. The autoclave was purged three times with ethylene before 90 mL of toluene or naphthane was quickly added under vacuum. A solution of certain amount nickel complex in 10 mL of toluene or naphthane was quickly injected into the reactor through a dry syringe under vigorous stirring. And then, the reactor was quickly filled in ethylene and kept at required pressure. After reaction for a desired period, stirrer was stopped, and the remaining ethylene was allowed to exhaust. The resultant polymer was filtered, washed several times with ethanol, and dried in a vacuum drying oven for 8 h at 70 °C.

Copolymerization Procedure. For all the copolymerization experiments, a 100-mL steel autoclave charged with a magnetic stirrer maintained at required temperature after heating under vacuum for 6 h at 130 °C. The autoclave was purged three times with ethylene before 30 mL of toluene added under ethylene atmosphere. A solution of comonomer in 10 mL of toluene and fresh catalyst solution in 10 mL of toluene were added in sequence under ethylene atmosphere. Ethylene was quickly filled in the autoclave and kept at required pressure. After the prescribed reaction time, the stirrer was stopped, and the remaining ethylene was allowed to exhaust. The solid copolymer was collected by filtration after precipitation from ethanol or methanol, washed with acetone, dried in a vacuum drying oven for 8 h to constant weight at 70 °C.

Acknowledgements

The authors are grateful for subsidy provided by the National Natural Science Foundation of China (No. 21690071 and 21574097).

Keywords: catalyst design • electronic structure • ligand effects • nickel • polymerization

References

[1] a) A. Nakamura, S. Ito, K. Nozaki, *Chem. Rev.* **2009**, 109, 5215-5244; b) L. S. Boffa, B. M. Novak, *Chem. Rev.* **2000**, 100, 1479-1493; c) J. Y. Dong, Y. L. Hu, *Coord. Chem. Rev.* **2006**, 250, 47-65; d) H. L. Mu, L. Pan, D. P. Song, Y. S. Li, *Chem. Rev.* **2015**, 115, 12091-12137; e) I. Shingo, *Bull. Chem. Soc. Jpn.* **2018**, 91, 251-261; f) T. Chen., C. L. Chen, Angew. Chem. Int. Ed. 2019, doi.org/10.1002/anie.201814634; g) C. L. Chen, *ACS Catal.* **2018**, 8, 5506-5514; h) S. X. Zhou, C. L. Chen, *Science Bulletin* **2018**, *63*, 441-445.

[2] a) E. Drent, R. van Dijk, R. van Ginkel, B. van Oort, R. I. Pugh, *Chem. Commun.* **2002**, 744-745; b) T. Kochi, K. Yoshimura, K. Nozaki, *Dalton Trans.* **2006**, 25-27; c) K. M. Skupov, P. R. Marella, M. Simard, G. P. A. Yap, N. Allen, D. Conner, B. L. Goodall, J. P. Claverie, *Macromol. Rapid. Commun.* **2007**, 28, 2033-2038; d) B. P. Carrow, K. Nozaki, *J. Am. Chem. Soc.* **2012**, 134, 8802-8805; e) N. D. Contrella, J. R. Sampson, R. F. Jordan, *Organometallics* **2014**, 33, 3546-3555; f) R. Nakano, K. Nozaki, *J. Am. Chem. Soc.* **2015**, 137, 10934-10937; g) S. Akita, R. Nakano, S. Ito, K. Nozaki, *Organometallics* **2018**, 37, 2286-2296; h) W. Tao, S. Akita, R. Nakano, S. Ito, Y. Hoshimoto, S. Ogoshi, K. Nozaki, *Chem. Commun.* **2017**, 53, 2630-2633; i) S. Y. Dai, C. L. Chen, *Macromolecules* **2018**, 51, 6818-6824; j) Y. N. Na, S. Y. Dai, C. L. Chen, *Macromolecules* **2018**, 51, 4040-4048; k) H. B. Hu, H. Y. Gao, L. Zhong, Q. Wu. *Polym. Chem.*, **2016**, 7, 529-537.

[3] a) T. Kochi, S. Noda, K. Yoshimura, K. Nozaki, *J. Am. Chem. Soc.* **2007**, 129, 8948-8949; b) S. Luo, J. Vela, G. R. Lief, R. F. Jordan, *J. Am. Chem. Soc.* **2007**, 129, 8946-8947; c) W. Weng, Z. Shen, R. F. Jordan, *J. Am. Chem. Soc.* **2007**, 129, 15450-15451; d) H. Yasuda, R. Nakano, S. Ito, K.

Nozaki, *J. Am. Chem. Soc.* **2018**, 140, 1876-1883; e) Z. Chen, W. Liu, O. Daugulis, M. Brookhart, *J. Am. Chem. Soc.* **2016**, 138, 16120-16129.

[4] a) L. Zhong, G. Li, G. Liang, H. Gao, Q. Wu, *Macromolecules* **2017**, 50, 2675-2682; b) B. K. Long, J. M. Eagan, M. Mulzer, G. W. Coates, *Angew. Chem. Int. Ed.* **2016**, 55, 7106-7110.

[5] M. Chen, C. Chen, *ACS Catal.* **2017**, 7, 1308-1312.

[6] a) T. R. Younkin, E. F. Conner, J. I. Henderson, S. K. Friedrich, R. H. Grubbs, D. A. Bansleben, *Science* **2000**, 287, 460-462; b) M. R. Radlauer, A. K. Buckley, L. M. Henling, T. Agapie *J. Am. Chem. Soc.* **2013**, 135, 3784-3787; c) D. Takeuchi, Y. Chiba, S. Takano, K. Osakada, Angew. Chem., Int. Ed. 2013, 52, 12536;

[7] a) S. Mecking, *Angew. Chem. Int. Ed.* **2001**, 40, 534-540; b) U. Klabunde (DuPont), USA 4698403, **1987** [Chem. Abstr. **1988**, 108, 151134w]; c) U. Klabunde, S. D. Ittel, *J. Mol. Catal.* **1987**, 41, 123**-**134; d) K. L. Makovetsky, E. S. Finkelshtein, V. I. Bykov, A. K. Bagdasaryan, B. L. Goodall, L. F. Rhodes, **1999**, WO 98/56837; e) U. Klabunde, R. Mulhaupt, T. Herskovitz, A. H. Janowicz, J. Calabrese, S. D. Ittel, J. Polym. Sci. Part A: *Polym. Chem.* **1987**, 25, 1989-2003.

[8] a) M. Chen, C. Chen, *Angew. Chem. Int. Ed.* **2018**, 57, 3094-3098; b) M. Li, X. Wang, Y. Luo, C. Chen, *Angew. Chem. Int. Ed.* **2017**, 56, 11604-11609; c) B. S. Xin, N. Sato, A. Tanna, Y. Oishi, Y. Konishi, F. Shimizu, *J. Am. Chem. Soc.* **2017**, 139, 3611-3614. d) Y. Konishi, W. J. Tao, H. Yasuda, S. Ito, Y. Oishi, H. Ohtaki, A. Tanna, T. Tayano, K. Nozaki, *ACS Macro Lett.* **2018**, 7, 213-217; e) X. Fu, L. J. Zhang, R. Tanaka, T. Shiono, Z. G. Cai, *Macromolecules* **2017**, 50, 9216-9221; f) W. J. Tao, R. Nakano, S. Ito, K. Nozaki, Angew. Chem., Int. Ed. 2016, 55, 2835-2839;

[9] Y. P. Zhang, H. L. Mu, L. Pan, X. L. Wang, Y. S. Li, *ACS Catal.* **2018**, 8, 5963-5976.

[10] a) H. L. Mu, W. P. Ye, D. P. Song, Y.S. Li, *Organometallics* **2010**, 29, 6282-6290; b) V. C. Gibson, A. Tomov, A. J. P. White, D. J. Williams, *Chem. Commun.* **2001**, 719-720; c) D. P. Song, W. P. Ye, Y. X. Wang, J. Y. Liu, Y. S. Li, *Organometallics* **2009**, 28, 5697-5704.

[11] a) A. Bastero, I. Göttker-Schnetmann, C. Röhr, S. Mecking, *Adv. Synth. Catal.* **2007**, 349, 2307-2316; b) M. A. Zuideveld, P. Wehrmann, C. Rohr, S. Mecking, *Angew. Chem. Int. Ed.* **2004**, 43, 869-873.

[12] R. Soula, J. P. Broyer, M. F. Llauro, A. Tomov, R. Spitz, J. Claverie, X. Drujon, J. Malinge, T. Saudemont, *Macromolecules* **2001**, 34, 2438-2442.

[13] a) M. P. Weberski, Jr.; C. L. Chen; M. Delferro; C. Zuccaccia; A. Macchioni; T. J. Marks, *Organometallics* **2012***,* 31, 3773-3789; b) M. P. Weberski, Jr.; C. L. Chen; M. Delferro; T. J. Marks, *Chem. Eur. J.* **2012***,* 18, 10715-10732; c) C. Popeney; Z. B Guan, *Organometallics* **2005**, 24, 1145-1155; d) H. Y. Gao; Z. F. Ke; L. X. Pei; K. M. Song; Q. Wu, *Polymer* **2007**, 48, 7249-7254.

[14] a) C. S. Popeney; C. M. Levins; Z. B. Guan, *Organometallics* **2011**, 30, 2432-2452; b) X. H. Hu; S. Y. Dai; C. L. Chen, *Dalton Trans.* **2016**, 45, 1496-1503; c) L. H. Guo; S. Y. Dai; C. L. Chen, *Polymers* **2016**, 8, 1-10.

[15] J. Heinicke, M. Köhler, N. Peulecke, M. He, M. K. Kindermann, W. Keim, G. Fink, *Chem. Eur. J.* **2003**, 9, 6093-6107.

[16] A. Berkefeld, M. Drexler, H. M. Moeller, S. Mecking, *J. Am. Chem. Soc.* **2009**, 131, 12613-12622.

[17] J. Wang, E. Yao, Z. Chen, Y. Ma, *Macromolecules* **2015**, 48, 5504-5510.

[18] F. S. Liu, H. B. Hu, Y. Xu, L. H. Guo, S. B. Zai, K. M. Song, H. Y. Gao, L. Zhang, F. M. Zhu, Q. Wu, *Macromolecules* **2009**, 42, 7789-7796.

[19] a) P. Wucher, V. Goldbach, S. Mecking, *Organometallics* **2013**, 32, 4516-4522; b) P. Kuhn, D. Sémeril, C. Jeunesse, D. Matt, M. Neuburger, A. Mota, *Chem. Eur. J.* **2006**, 12, 5210-5219. c) J. X. Gao; B. P. Yang; C. L. Chen, *J. Catal.* 2019, 369, 233-238.

[20] M. Peuckert, W. Keim, *Organometallics* **1983**, 2, 594-597.

[21] a) D. P. Gates, S. A. Svejda, E. Oñate, C. M. Killian, L. K. Johnson, P. S. White, M. Brookhart, *Macromolecules* **2000**, 33, 2320-2324; b) Z. Chen, M. Mesgar, P. S. White, O. Daugulis, M. Brookhart, *ACS Catal.* **2015**, 5, 631-636; c) D. W. Wan, Y. S. Gao, J. F. Li, Q. Shen, X. L. Sun, Y. Tang, *Dalton Trans.* **2012**, 41, 4552-4557; d) H. S. Schrekker, V. Kotov, P. Preishuber-Pflugl, P. White, M. Brookhart, *Macromolecules* **2006**, 39, 6341-6354.

[22] a) J. L. Rhinehart, L. A. Brown, B. K. Long, *J. Am. Chem. Soc.* **2013**, 135, 16316-16319; b) J. L. Rhinehart, N. E. Mitchell, B. K. Long, *ACS Catal.* **2014**, 4, 2501-2504; c) T. Xie, K. B. McAuley, J. C. C. Hsu, D. W. Bacon, *Ind. Eng. Chem. Res.* **1994**, 33, 449-479.

[23] a) P. Wucher, P. Roesle, L. Falivene, L. Cavallo, L. Caporaso, I. Göttker-Schnetmann, S. Mecking, *Organometallics* **2012**, 31, 8505-8515; b) D. Guironnet, P. Roesle, T. Rüenzi, I. Göettker-Schnetmann, S. Mecking, *J. Am. Chem. Soc.* **2009**, 131, 422-423.

10.1002/cctc.201900265

WILEY-VCH

Entry for the Table of Contents

FULL PAPER

Newly synthesized bulky nickel complexes are thermally robust, and exhibits very high activity (up to 10^7 $g \cdot mol_{Ni}^{-1} \cdot h^{-1}$) in ethylene polymerization even at 120 °C, and these complexes bearing electron-withdrawing substituents on *ortho*-phenoxy position or electron-donating substituents on phosphorus atom show higher activity than contrastive catalyst toward ethylene polymerization and ethylene–methyl acrylate (MA) copolymerization.

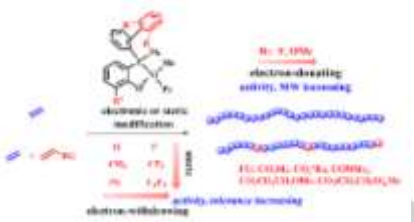

Yanping Zhang, Hongliang Mu, Xuling Wang, Li Pan, Yuesheng Li**

Page No. – Page No.

Elaborate Tuning in Ligand Makes Big Differences in Catalytic Performance: Bulky Nickel Catalysts for (Co)polymerization of Ethylene with Promising Vinyl Polar Monomers